DNA photoproducts released by repair in biological fluids as biomarkers of the genotoxicity of UV radiation

Noémie Reynaud, Laura Belz, David Béal, Daniel Bacqueville, Hélène Duplan, Camille Genies, Emmanuel Questel, Gwendal Josse, Thierry Douki

DNA photoproducts released by repair in biological fluids as biomarkers of the genotoxicity of UV radiation

Noémie Reynaud[1], Laura Belz[1], David Béal[1], Daniel Bacqueville[2], Hélène Duplan[2], Camille Géniès[2], Emmanuel Questel[3], Gwendal Josse[3], Thierry Douki[1*]

1 Univ. Grenoble Alpes, CEA, CNRS, IRIG, SyMMES, F-38000 Grenoble, France

2 Service Recherche Pharmaco-Clinique, Département Recherche Appliquée, Centre R&D Pierre Fabre, F-31000 Toulouse, France

3 Centre de Recherche sur la Peau, Pierre Fabre Dermo-Cosmétique, F-31000 Toulouse, France

* Corresponding author:

Thierry Douki

ORCID: 0000-0002-5022-071X

Email : thierry.douki@cea.fr

Tel (33) 4 38 78 31 91

ABSTRACT

UV-induced formation of photoproducts in DNA is a major initiating event of skin cancer. Consequently, many analytical tools have been developed for their quantification in DNA. In the present work, we extended our previous liquid chromatography – mass spectrometry method to the quantification of the short DNA fragments containing photoproducts that are released from cells by the repair machinery. We designed a robust protocol including a solid phase extraction step (SPE), an enzymatic treatment aimed at releasing individual photoproducts, and a liquid chromatography method combining on-line SPE and ultra-high performance liquid chromatography for optimal specificity and sensitivity. We also added relevant internal standards for a better accuracy. The method was validated for linearity, repeatability and reproducibility. The limits of detection and quantification were found to be in the fmol range. The proof of concept of the use of excreted DNA repair products as biomarkers of the genotoxicity of UV was obtained first in *in vitro* studies using cultured HaCat cells and *ex-vivo* on human skin explants. Further evidence were obtained from the detection of pyrimidine dimers in the urine of human volunteers collected after recreational exposure in summer.

Keywords: Biomarkers, Biological fluids, UHPLC-MS/MS, Solid phase extraction, DNA damage

GRAPHICAL ABSTRACT

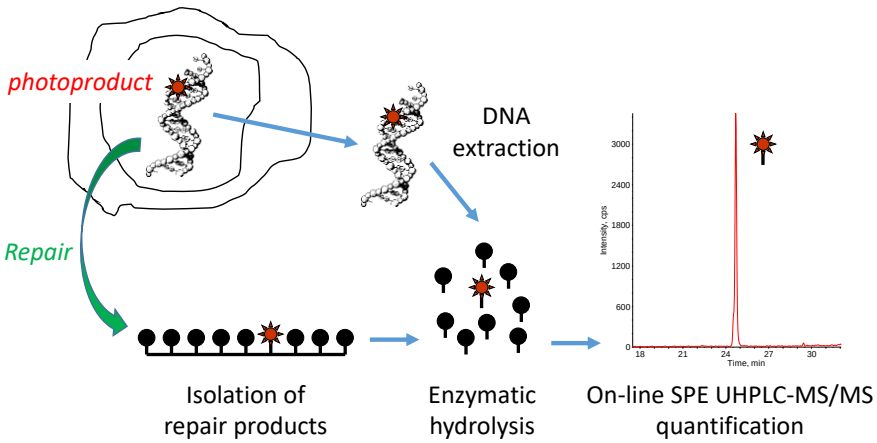

An assay was designed to quantify the DNA photoproducts released from cells within short fragments by the DNA repair machinery. These oligonucleotides were isolated by solid phase extraction and enzymatically hydrolyzed. The photoproducts were then quantified by on-line SPE combined with UHPLC-MS/MS with isotopic dilution.

INTRODUCTIION

Overexposure to solar and artificial ultraviolet radiation (UV) exhibits major deleterious effects on living systems. In humans, UV are responsible for photoaging, erythema, immunosuppression and skin cancers (1-3). The ability of UV at inducing cutaneous tumors is mostly explained by their DNA damaging and mutational properties (4, 5). A number of experimental evidence have shown that UVB (280-320 nm) is the most damaging portion of the solar spectrum (6-8). Absorption in this wavelength range induces photoreactions and leads to the formation of pyrimidine dimers (***Erreur ! Source du renvoi introuvable.***) (5, 9, 10). Those include *cis,syn* cyclobutane pyrimidine dimers (CPD *c,s*), pyrimidine (6-4) pyrimidone photoproducts (64PP) and their Dewar valence isomers (Dewar) for the four possible bipyrimidine sequences (TT, TC, CT and CC). UVA (320-400 nm) is at least 20 times more intense than UVB in sunlight but is 2 to 3 orders of magnitude less efficient at damaging DNA (11-13). Consequently, emphasis has been placed on UVB-induced pyrimidine dimers for *in vitro* and *in vivo* studies.

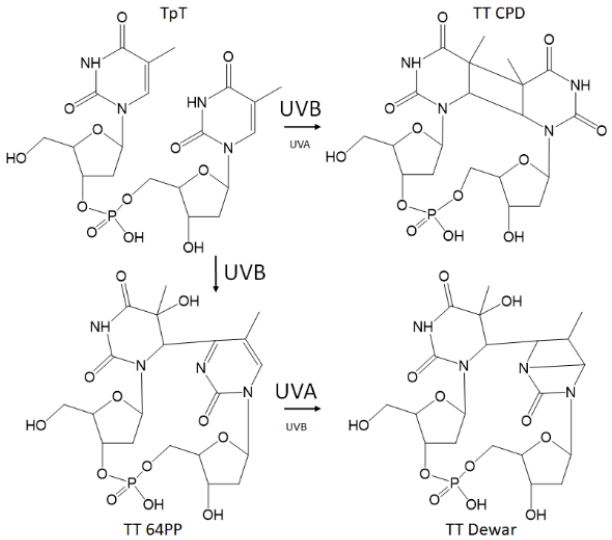

Scheme 1: Chemical structure of UV-induced pyrimidine dimers. The scheme shows photoproducts produced at TT sites. Similar photoreactions also take place at TC, CT and CC

sequences. The compounds are shown in the form of modified dinucleoside monophosphates as used for their detection in the present work.

For carrying out photochemical and photobiological studies on pyrimidine dimers, a wide variety of analytical approaches has been proposed over the years. The challenge is the low level of modification in biological samples (less than 1 photoproduct per 10^5 or 10^6 normal bases) and the small amount of material available (a few µg of DNA in a skin biopsy). Currently, the most widely applied assays are immunological techniques (14, 15) and chromatographic detection (9). The former are based on the production of monoclonal or polyclonal antibodies raised against dimers that can be used by immunohistochemistry in tissue samples but also by either immuno-dot blot in extracted DNA or flow cytometry in cell suspensions. Chromatographic assays require DNA extraction and hydrolysis into monomers. A chromatographic separation of the mixture followed by adequate specific and sensitive detection provides quantitative data. The main advantage of this class of methods is that it can provide individual information on all possible pyrimidine dimers, in contrast to immunological assays that detect each type of photoproduct without sequence specificity. Early chromatographic works have used radioactive labeling of DNA (16), fluorescence (17) and ^{32}P-post labeling (18, 19). The most currently used chromatographic techniques rely on mass spectrometry coupled to either gas phase (20) or liquid chromatography (9, 21, 22). The latter type of assay developed in our group (23, 24) is based on the coupling of high performance liquid chromatography to triple quadrupolar mass spectrometry with electrospray ionization (HPLC-MS/MS).

Results from the literature suggest that pyrimidine dimers present in biological fluids as the result of DNA repair could be an interesting target in addition to nuclear DNA. First, the presence of TT CPD *c,s* in urine of exposed volunteers was shown by ^{32}P-post labeling detection

(25-27). In addition, the oligonucleotides bearing a photoproduct that are produced upon nucleotide excision repair (NER) were detected in cultured cells, where they are digested by in shorter fragment (28). From there, they can be isolated and used as marker of formation of DNA damage and repair (29-32). A similar *ex-vivo* observation was made in skin explants that were shown to harbor photoproducts-containing oligonucleotides after exposure to UV (33). A recent work also observed release of photoproducts from cultured cells in the culture medium (34). However, those are located in DNA fragments embedded in vesicles and that are much larger than the repair products resulting from NER. Moreover, the concentration of this specific class of photoproducts increases in the culture medium of repair-deficient cells. Altogether, these photoproducts cannot be considered as released by NER.

In the present work, we hypothesized that the actual photoproduct-containing oligonucleotides released by NER (rep-oligos) are excreted from cells into biological fluids or culture media. We designed an assay for the detection of the pyrimidine dimers they contain in easily accessible biological fluid like urine for *in vivo* studies and cell culture medium for *in vitro* investigations. Emphasis was placed on the most frequent photoproduct, TT CPD *c,s*, and the photoproduct detected with the highest sensitivity by MS/MS, namely TT 64PP. A solid phase extraction (SPE) step was optimized for the isolation of rep-oligos. We also developed an isotopic dilution approach and used ultra-high performance liquid chromatography (UHPLC) combined with on-line SPE. The second part of the work was devoted to the biological validation of the concept of the use of excreted repair products as biomarkers of exposure to UV. This was performed *in vitro* in cultured HaCat cells, *ex-vivo* in human skin explants and in urine from exposed human.

MATERIAL AND METHODS

Chemicals and enzymes

Reagents

Methanol (MeOH) >99.9 % purity (CHROMASOLV grade) was purchased from Sigma-Aldrich and LC-MS grade acetonitrile (ACN) from Carlo Erba. Triethylammonium acetate (TEAA, 1 M in water), tris(hydroxymethyl)aminomethane (Tris), ethylene diamine tetraacetic acid (EDTA), sucrose, Triton-X100, sodium dodecyl sulfate (SDS), chloroacetaldehyde and 1,N^6-etheno-2'-deoxyadenosine (εdAdo) were from Sigma (Saint-Quentin-Fallavier, France). Reagents and solvents for synthesis (5'-dimethoxytrityl-3'-phosphoramidite-thymidine, dimethoxytrityl chloride, acetic anhydride, acetic acid, pyridine, ethyl-*S*-triazol, iodine, ammonium hydroxide) were of the highest purity available and purchased form Aldrich (Saint-Quentin-Fallavier, France). ($^{13}C_{10}$, 98% $^{15}N_2$, 96-98%)-thymidine was from Cambridge Isotope Laboratories. [$^{15}N_5$]-εdAdo was synthetized as previously reported (35). Thymidylyl-(3'-5')-thymidine (TpT) was prepared by phosphodiester synthesis and all photoproducts of dinucleoside monophosphates were obtained as previously reported (23).

Synthetic oligonucleotides

Oligonucleotides (HPLC purified grade) were purchased from Eurogentec (Angers, France). For SPE optimization and preparation of UV-irradiated oligonucleotides (oligo-UV), a 15-mer (CATCTTACATTTTAC) and a 5-mer (TCTTA) were used. The UV irradiated oligonucleotides were obtained by exposure of 0.2 mg ml^{-1} solutions to UVC radiation for 30 min. The resulting mixtures were calibrated for their content in photoproducts by HPLC-MS/MS following enzymatic hydrolysis as detailed below. When used in quality control samples (QC), the two solutions were mixed. For the synthesis of oligonucleotides bearing

ethenoadenine bases (oligo-εdAdo), solutions of a 5-mer (ATTGC), a 10-mer (TATTGTTGCA), a 15-mer (CATTGTATTGTTGCA) and a 20-mer (ATTGTATTGTATTGATTGCAA) were individually prepared in concentration corresponding to 0.1 mM adenine. The solutions (500 µL each) were mixed and treated overnight with chloroacetaldehyde (10 mM). The oligonucleotides were purified and the solution was calibrated for the content in εdAdo by HPLC-MS/MS.

Synthesis of [M+12]-photoproducts

We first synthesized a [M+12] labelled derivative of TpT. The first step was the condensation of 3'-end protected [$^{13}C_{10}$,$^{15}N_2$]-thymidine to a 5' end thymine phosphoramidite synthon. The resulting compound was oxidized into dinucleoside monophosphate and deprotected in acidic and alkaline conditions. The water-soluble fraction of the reaction mixture was purified by reverse phase HPLC (C18 column, 4x250 mm ID, TEAA/ACN gradient, flow rate 1 ml min^{-1}) with UV detection at 230 nm. A fraction containing the expected product was isolated, concentrated and purified a second time. It was then characterized by UHPLC analysis with UV and MS1 mass spectrometry detection (see chromatographic conditions below). The isolated product was further identified by detection in the product ion scan mode (MS^2) by comparison with unlabeled TpT. All fragments were identical in both cases with the exception of shifts in m/z explained by the presence of ^{13}C or ^{15}N atoms . An aqueous solution of [M+12]-TpT was then exposed to UVC to yield dimeric photoproducts. The extent of modification of [M+12]-TpT during irradiation was monitored and the irradiation was stopped when the yield of TT CPD *c,s* reached a plateau as the result of the UVC-induced reversion. The irradiated solution was then purified on a reverse phase HPLC system with UV detection (230 nm) and the fraction containing the photoproducts was isolated. Photoproducts were characterized by UHPLC with MS^2 detection. The content in TT CPD *c,s*, 64PP and Dewar was

determined by HPLC-MS/MS with detection in the MRM mode. An external calibration using unlabeled standards was used.

Enzymes

Proteinase K and protease were purchased from Qiagen (Courtaboeuf, France). Phosphodiesterase II was from Worthington (Lakewood, NJ). RNase A, RNase T1, DNase II, nuclease P1, alkaline phosphatase and phosphodiesterase I were purchased from Sigma (Saint-Quentin-Fallavier, France).

Solid phase extraction and enzymatic hydrolysis

The optimized SPE protocol for the quantification of TT CPD *c,s* and TT 64PP in biological fluids included several steps. First, oligo-εdAdo was added (2.5 µL, 100 nM εdAdo) to typically 200 µL of urine or 400 µL of culture medium. Ten or 40 µL of 1 M TEAA was added, respectively. The sample was deposited on top of a HRX-100 (45 µm particle size, 100 mg phase) SPE column (Macherey-Nagel, Gutenberg, France) conditioned with a 50 mM aqueous solution of TEAA. The liquid was removed under vacuum and the column washed with 1 mL of buffer (15% MeOH+85% of aqueous solution of 50 mM TEAA). The elution was then performed with 1 mL of a mixture of MeOH (75%) and 50 mM TEAA (25%). After evaporation of MeOH in a speed-vac (model SPD 111V, Savant, Thermo Scientific) and of water by freeze-drying in an Alpha 1-2 system (Christ), the obtained residue was solubilized in 100 µL of a solution containing [M+12]-TpT photoproducts (5 nM TT CPD *c,s* and 3.5 nM TT 64PP) and 5 nM [M+5]-εdAdo. The resulting solution was enzymatically hydrolyzed in two steps as previously described (36). Briefly, the sample was first incubated for 2h at pH 5.5 with nuclease P1, phosphodiesterase II and DNase II. The pH was raised to 8 by addition of Tris buffer and the hydrolysis was resumed for 2h in the presence of alkaline phosphatase and phosphodiesterase I. The resulting solution was filtered at 0.2 µm and transferred into HPLC

vials. Quality control samples were prepared by mixing oligo-εdAdo (2.5 µL, 100 nM) to a solution of oligo-UV (2.5 µL at 100 nM in TT CPD *c,s* and 52 nM in TT 64PP). The mixture was freeze-dried and treated by using the protocol applied to SPE-purified samples.

Liquid chromatography-tandem mass spectrometry analyses

Preparation of the calibration curve

The samples for the calibration curve were prepared by mixing increasing volumes (0, 1, 2 and 5 µL) of a mixture of TpT photoproducts at 100 nM and of a solution of εdAdo (0, 1, 2 and 5 µL at 100 nM) in HPLC vials. The samples were then freeze-dried and further solubilized in 100 µL of the solution of isotopically labeled internal standard (50 nM [M+12]-TpT photoproducts and 50 nM [$^{15}N_5$]-εdAdo. The same solution was used for the solubilization of the SPE-purified samples and the QC.

Liquid chromatography

Chromatographic separations were performed on a ExionLC AD series chromatographic system (SCIEX, Framingham, MA) equipped with an octadecylsilyl silica gel on-line SPE column (Nucleodur C18 Gravity, 5 µm particle size, 2×50 mm ID, Macherey-Nagel, Gutenberg, France) and a mixed pentafluorophenyl (PFP) / C18 silica gel analytical column (Excel C18-PFP, 1.7 µm particle size, 2.1×100 mm ID, ACE, Aberdeen, UK). The on-line SPE part of the system consisted in two pumps, an autosampler and a 6-ways valve located in the column oven (temperature 30°C). The on-line C18 SPE column was connected to the outlet of the autosampler and to one inlet of the 6-ways valve. The gradient first ranged from 0 to 10% ACN in 20 mM TEAA in 1 min at a flow rate of 400 µL min^{-1}. The 6-ways valve was commuted from the "load" to the "inject" position 1 min after injection of the sample. In this configuration, the mobile phase in the SPE column was provided by two pumps of the analytical part of the

chromatographic system. After 4 min, the valve was switched back to the "load" position, and the SPE column was rinsed by 50% ACN between 6 and 8 min before being equilibrated in pure 20 mM TEAA. Meanwhile, the purified sample was eluted in the PFP-C18 analytical column. The flow rate was 200 µL min^{-1}. Solvent A was 5 mM TEAA and solvent B 20% ACN in 5 mM TEAA. The gradient was left at 10% B for 1 minute and then linearly increased to 45 % until 9 min. The proportion of B increased then to 100 % within 7 min and the mobile phase was maintained at this composition for 1 min. At the outlet of the analytical column, the flow passed through a diode array UV detector (220-320 nm) used to quantify normal nucleosides in DNA samples by external calibration. The outlet was then directed toward the mass spectrometer.

Mass spectrometry

The mass spectrometer was a 6500+ QTrap apparatus (SCIEX, Framingham, MA). In the first part of the analysis (9 min), it was operated in the negative electrospray ionization mode for the detection of the photoproducts. Then, the polarity was then changed to positive until the end of the run (20 min) for the detection of εdAdo. Source parameters were optimized to reach the best compromise for the different analytes. In the negative mode, the nitrogen pressure of curtain gas, ion source gas 1 (nebulization) and ion source gas 2 (heated sheath gas) were set at 45, 60 and 60 psi respectively. The collision gas was set at High. The ion spray voltage was -4300 V and the source temperature 550°C. The exhaust gas (air) was set at 25 L min^{-1}. The dwell time was 50 ms for all transitions. For the positive ionization detection of εdAdo, curtain gas, ion source gas 1, ion source gas 2, collision gas, ion spray voltage and source temperature were set at 45 psi, 60 psi, 60 psi, High, 5000 V and 550°C, respectively. In this period, the dwell time was 400 ms. Detection was made in the "multiple reaction monitoring mode" (MRM) in which the signal corresponding to fragmentation reactions specific to each analyte are quantified. Three MRM transitions were used for TT CPD *c,s* and TT 64PP and

only one for εdAdo that underwent only loss of the deoxyribose unit. (see Electronic Supplementary Material Table S1).

Expression of the results

Following SPE purification, all samples were resuspended in 100 µL as mentioned in SPE section. In all cases, the injection volume was 50 µL. Calibration curves and correction with the oligo-εdAdo internal standard provided accurate concentrations expressed in nM of the injected solution. In some cases, a correction factor was applied when the initial volume of the biological sample was different from 100 µL. For example, factors 2 or 4 were applied for 200 µL urine or 400 µL medium or cytoplasmic fraction.

Biological Samples

Collection of human urines

For all studies, only healthy volunteers were recruited. This work was performed in the framework of cosmetic-oriented studies that, according to the French legislation, do not require declaration to an ethic committee. However, urine collection was performed in an approved center, in compliance with the Declaration of Helsinki (1964) and its subsequent revisions, and in the spirit of Good Clinical Practice. All samples were anonymized before analysis. The first study was carried out in winter and volunteers were asked not expose themselves to excess natural sunlight or artificial UV. Urine (78 samples) was collected on 17 different days over a period of 47 days, except for one donor for which only 10 samples could be obtained. A second study was designed to provide another set of samples consisted in urines collected from three volunteers 2 days after the end of their summer vacations during which normal photoprotection and exposure habits were followed. Samples (100 µL) were purified by SPE and analyzed by on-line SPE/UHPLC-MS/MS.

Cell culture and human explants

HaCat cells were grown in GlutaMAX™ Dulbecco's Modified Eagle Medium (Gibco) medium supplemented with 10% (v/v) fetal calf serum (Gibco). A mixture of antibiotics (50 U/mL of penicillin and 50 mg/mL of streptomycin) was added in a 1% (v/v) proportion. Cells were seeded at 3×10^5 mL^{-1} in 35 mm diameter petri dishes with 2 mL medium. They were grown in an incubator (Hera Cell, Heraeus) at 37°C in a 5% CO_2 atmosphere until 70% confluency and used for irradiation.

Human skin samples were obtained following breast surgery from heathy female donors (Centre Hospitalier Universitaire de Grenoble, Grenoble, France). All experiments were performed in accordance with relevant guidelines and regulations. In particular, work was performed in agreement with article L1245-2 of the French Public Health Code on the use of surgical wastes for research purposes. It stipulates that donors must be informed and agree, and that samples are used anonymously. Collection and storage of human skin samples was declared to the French authorities and validated in the CODECOH DC-2008-444 document. All donors were of skin phototype II or III, according to the Fitzpatrick classification. Immediately after collection, 0.25 mm thick epidermal layer was isolated by using a SOBER hand-held dermatome (Humeca, Enschede, Netherlands). Twelve-mm punch biopsies were then prepared with sterile punches (Help Medical, France). They were placed with the dermal side down into ThinCert™ inserts (Greiner Bio-One, Austria) maintained in 12 well cell culture plates (Greiner Bio-One, Austria). The explants were maintained at the liquid/air interface in DMEM/F-12 medium (Thermo-Fisher) containing 10% Pen/ Strep at 37 °C in a humidified incubator containing 5% CO_2.

Irradiations

All irradiations were performed with a LS1000 Solar Simulator (Solar Light Company, Glenside, PA) that emitted 5% UVB and 95% UVA. Simulated sunlight (SSL) doses are

expressed in “minimal erythemal doses” (MED), with 1 MED corresponding to 4 J cm^{-2} h^{-1} with our equipment. Irradiations were performed with the samples placed in PBS in order to avoid photosensitization by components of the culture medium. Two different protocols were used and referred to as “cumul” and “renew” (**Erreur ! Source du renvoi introuvable.**). In the “cumul” protocol, a number of samples equal to the number of doses and time points to be investigated were prepared. After irradiation, samples were collected at each time point and both cells and medium are collected. Therefore, each sample reflected the cumulative effect from exposure to a defined post-irradiation time. In the “renew” protocol, a lower number of samples were prepared and varied only in the SSL dose applied. At different post-irradiation times, the medium was collected but the *in vitro* model investigated (cells or explant) was left intact. Fresh medium was added and the incubation resumed. At the last time point, both cells and cultured medium were collected. In this protocol, the total amount of released photoproducts is obtained by summation of the values determined at the different time points. All experiments with HaCat cells were carried out in triplicates, and each experiments was repeated at least two or three times. Work with skin explants was performed once in triplicate because of the limited availability of this type of samples.

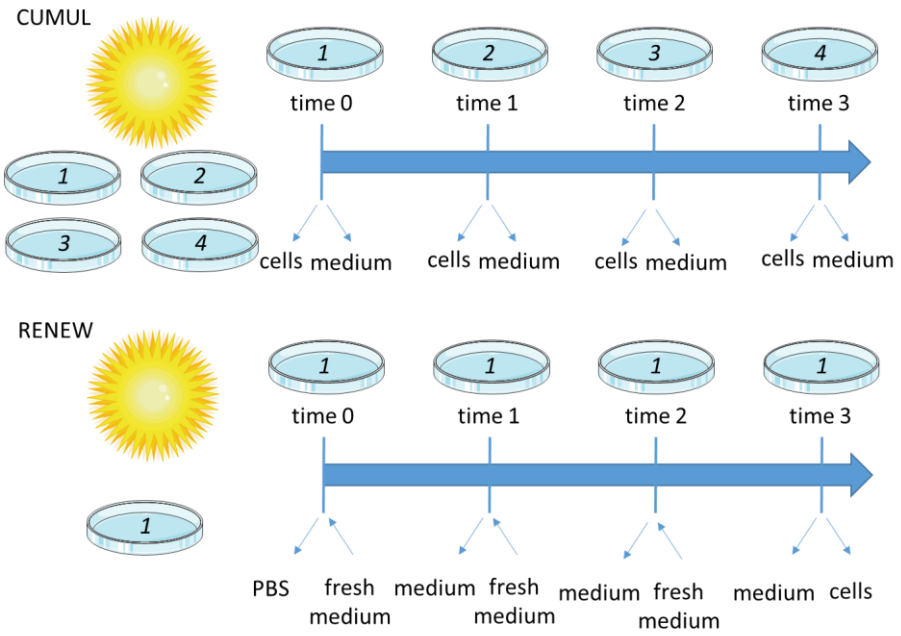

Scheme 2: Principle of the two protocols used for the follow—up of the time-dependent evolution of the amounts of photoproducts in cells and culture medium. In the "cumul" protocol, one cell culture was used for each time point while in the "renew" protocol, only one culture was used and the medium collected and replaced at different time points.

DNA extraction and hydrolysis

DNA was extracted from cells as previously described (37). The cell pellet first underwent lysis in a buffer containing Tris, EDTA, sucrose and Triton X-100 as surfactant. Nuclei were isolated by centrifugation and lyzed in a second buffer containing Tris, EDTA and SDS. After incubation with RNase A, RNase T1 and protease, DNA was precipitated by a mixture of NaI and isopropanol. DNA was extracted from explant by using the DNeasy kit from Qiagen. Samples were first mechanically disrupted with steel beads in a TissuLyzer (Qiagen) in AL buffer (Qiagen). Proteinase K was added and the samples incubated à 50°C for 3 h. RNaseA was added and the sample left at room temperature for 2 min. ATL Buffer (Qiagen) was added and the samples placed at 70°C for 10 min. After cooling, ethanol was added and the samples were eluted in a DNA-retaining column (Qiagen). After two washing steps, DNA was eluted in pure water. The samples were freeze-dried overnight. DNA hydrolysis was then performed as

described above for SPE-purified rep-oligos. The samples were filtered and transferred into HPLC vials.

Isolation of rep-oligos from cytoplasmic fractions

In HaCat experiments, the collected cell pellets were divided in two equal fractions. One was used for DNA extraction as described above and the other for the isolation of rep-oligos from the cytoplasmic fraction. For this purpose, a lysis of the cells was carried out with a N-(2-hydroxyethyl)piperazine-N′-(2-ethanesulfonic acid (HEPES) buffer (200 µL) containing $MgCl_2$, KCl and 0.01% of Triton X-100. The cells were lysed by a series of freezing / thawing steps. The obtained solution was filtered first through a 0.2 µm nylon membrane (ultrafiltration centrifuge units, VWR) and then through a 30 kDa cut-off modified polyethersulfone membrane (NanoSEP, PALL Life Sciences) to remove any traces of nuclear DNA. Rep-oligos were then isolated by solid phase extraction as described above for urines and culture medium.

Statistical analyses

ANOVA analysis with Fisher test of the intra- and inter-day variability was performed by one factor analysis of variance with the statistical analysis tool of the excel software (Microsoft, Redmond, WA). Statistical significance of the time and dose effects in the biological experiments was assessed through a Kruskal-Wallis test followed by a Dunn's test for multiple comparisons. The analyses were performed with the Prism 9 software (GraphPad, San Diego, CA).

RESULTS AND DISCUSSION

The aim of the present work was to develop an assay for the quantification of the photoproduct-bearing oligonucleotides (rep-oligos) released by the DNA repair machinery into biological media. The protocol was designed in three steps including the SPE-based isolation of the oligonucleotides, their enzymatic hydrolysis and the quantification of the released photoproducts by an on line-SPE/UHPLC-MS/MS method with isotopic dilution. *In vitro*, e*x-vivo* and human studies were performed to validate the biological relevance of this new class of biomarkers.

Optimization of the analytical protocol

SPE purification and hydrolysis of the oligonucleotides

The purpose of the first step of the protocol is to isolate rep-oligos from the biological fluids. For this purpose, we chose to use the robust and widely applied solid phase extraction approach (38, 39). Our experience on other DNA models and on dimeric photoproducts led us to select columns packed with hydrophobic solid phases. Optimization was carried out with synthetic oligonucleotides that were either 15 or 5 nucleotides-long. This range of sizes was expected to mimic repair products released from cells after partial degradation by nucleases (28). In all experiments, elution was performed with aqueous solutions containing TEAA in various concentrations and methanol in various proportions. TEAA was used as a buffer because it forms ion pairs with the phosphate group of oligonucleotides and increases their retention time and improves peak shape.

In a first series of experiments, oligonucleotides were deposited on top of the SPE columns and eluted with fractions containing increasing proportion of MeOH (typically 5, 10, 20, 30, 50, 75

and 100 %). Efficiency of the SPE purification was estimated by quantifying oligonucleotides by HPLC-MS/MS in solution before and after purification (data not shown). We observed a better recovery on a polymeric phase (polystyrene-divinylbenzene copolymer) than an octadecylsilyl silica gel column (see Electronic Supplementary Material Fig. S1). For the former, we obtained similar results with columns containing 100 and 200 mg support. In order to optimize the elution parameters, we mostly worked with urine, the most complex matrix we intended to investigate. In this experiment, the sample volume was 100 µl and the SPE column contained 100 mg HRX resin. All elution solutions contained 20 mM TEAA. We observed that oligonucleotides were less retained on the SPE column when applied in urine than in plain water (see Electronic Supplementary Material Fig. S2a), with risk of losing material in washing step. In order to prevent this phenomenon, we added concentrated TEAA to the urine sample to favor ion pairing prior to deposition onto the column. Addition of TEAA proved to be efficient at 50 mM since no oligonucleotide was eluted in fractions containing less than 30% MeOH. At 100 mM, a significant proportion of the oligonucleotides was still present at 75 % MeOH, which could be a sign that the product was partially trapped in the column (see Electronic Supplementary Material Fig. S2b). We thus chose a protocol where the sample was adjusted to 50 mM TEAA, which has the additional advantage of controlling the pH. Washing and elution were performed with 50 mM TEAA solution containing 15 % and 75% MeOH, respectively. We also checked that this procedure did not lead to loss of the shortest possible form of DNA photoproduct, the dinucleoside monophosphate (data not shown). We obtained a 75 and 85 % recovery yield for the TT CPD *c,s* and 64PP, respectively.

Hydrolysis of the isolated oligonucleotides

In the following step, the isolated oligonucleotides were enzymatically hydrolyzed prior to HPLC-MS/MS analysis. The hydrolysis procedure, well optimized in our group (9), relies on a series of enzymes. In a first step carried out at pH 5.5, DNase II and nuclease P1 cleave long

genomic double-stranded DNA into shorter fragment. This shorter size of DNA facilitates the action of phosphodiesterase II that hydrolyzes DNA from its 5'-end and releases normal bases as 3'-nucleotides. When reaching sites with a photoproduct, phosphodiesterase II cannot remove the intradimer phosphate and bypasses the photoproduct, leaving a few normal nucleotides still linked to the released fragment. In the subsequent step carried out at pH 8, phosphodiesterase I hydrolyses DNA from the 3'-end and thus removes the normal nucleotides still attached to the photoproduct. Yet, it does not cleave the intradimer phosphate group. Alkaline phosphatase is used in this step to remove the phosphate groups of the normal nucleotides, thereby releasing nucleosides. The optimal efficiency of these enzymes is strongly dependent on the composition of the sample and in particular the pH. It was thus a major point to check that hydrolysis was not hampered by the possible traces of TEAA or components of urine present in SPE isolated fractions. This was not the case since photoproducts could be unambiguously be detected when oligo-UV mixed with either water, urine or culture medium were purified by SPE, freeze-dried, enzymatically hydrolyzed and analyzed by HPLC-MS/MS.

Liquid chromatography – tandem mass spectrometry analysis

After designing the SPE protocol, we determined the sensitivity of the HPLC-MS/MS assay for pyrimidine dimers in solution in purified urine. For this purpose, 200 µL of urine was submitted to the optimized SPE protocol. The final residue was solubilized in 100 µL of water and spiked with pure TpT photoproducts at increasing concentration. Similar dilutions were prepared with pure water. Comparison between the calibration curves obtained in urine and those determined in pure water showed the occurrence of a strong matrix effect. For a same injected amount, the signal was 2.5 times lower when the standard was diluted in urine than in water (**Erreur ! Source du renvoi introuvable.**). Accordingly, the signal of a same amount of standard was found to decrease when the volume of urine used in the SPE step increased (data not shown).

These results showed that the SPE step was not sufficient to yield quantitative results in the HPLC-MS/MS detection.

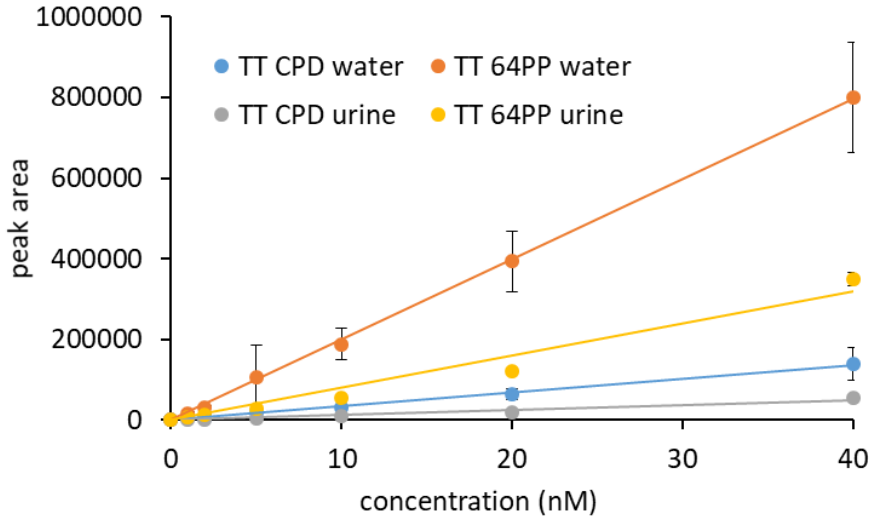

Figure 1: Comparison of the area of the peaks on the HPLC-MS/MS chromatograms for increasing amounts of photoproducts injected in solution either in water or in SPE-purified urine. The results are mean ± standard deviation for three independent analyses.

Internal standards

A first improvement of the assay was the use of isotopically labeled internal standards, an analytical approach widely used for quantification many biomarkers (40) and DNA damage (41). In its first applications (9, 23, 42), our HPLC-MS/MS assay for pyrimidine dimers did not use isotopic dilution because it was applied only to hydrolyzed isolated DNA. We checked that this matrix did not affect the MS/MS signal. This was no longer the case in urine. Therefore, we synthetized ^{13}C- and ^{15}N-enriched photoproducts of the targeted dinucleoside monophosphate TpT. A first step was the design of a synthesis strategy for the starting labeled TpT (see Electronic Supplementary Material Fig. S3). [$^{13}C_{10}$,$^{15}N_2$]-TpT was obtained in high purity. The latter was found to be 98% and 92% by HPLC-UV and HPLC-MS1 analyses, respectively (see Electronic Supplementary Material Fig. S4). Final structural identification was assessed from the MS^1 and MS^2 spectra (see Electronic Supplementary Material Fig. S5).

The MS^1 spectrum confirmed that the molecular weight of the isolated product was 558. Interestingly, unlabeled TpT could not be detected, which is a key point for isotopic dilution analyses. Fragmentation of the m/z=557 ion provided fragments similar to those produced by unlabeled TpT (24), with the exception of those with larger m/z because of the presence of stable isotopes. [M+12]-TpT was then exposed to UVC radiation to produce isotopically labeled photoproducts. A fraction containing the latter compounds was isolated by reverse phase HPLC under conditions providing efficient separation from unreacted [M+12]-TpT. UHPLC analysis with MS^2 detection provided unambiguous structural identification of the obtained photoproducts (see Electronic Supplementary Material Fig. S6). The pseudo-molecular ion was at m/z=557. A specific fragment corresponding to the loss of a dehydrated 2-deoxyribose moiety (98 amu) was observed for the [M+12]-TT CPD *c,s* as in the case of the unlabeled photoproduct (24). The fragmentation spectrum of [M+12]-TT 64PP exhibited a peak corresponding to the loss of a $C_4O_3NH_3$ moiety ($[M-113-H]^-$) arising from the rearrangement of the bases of the photoproduct. None of the lost carbon and nitrogen atoms was labeled as anticipated from the structure of the [M+12]-photoproduct. For both photoproducts, fragmentation products of the phosphodiester bond were also observed, in particular the ion at m/z=79 (phosphate) and 200 (phosphorylated $^{13}C_5$-deoxyribose) which are used in the MRM detection.

With these [M+12]-labelled internal standards in hand, we developed a MS/MS method with isotopic dilution in which each fragment of TT- CPD *c,s* and TT 64PP was associated with its labelled analog for the determination of the calibration curves. In methods involving a complex succession of sample preparation steps, internal standards also make possible to take into account the yield of extraction or purification. In our case, use of [M+12]-TpT photoproducts was not suitable because our SPE step did not aim at purifying the final analytes but longer DNA fragments that are subsequently hydrolyzed to release the photoproducts as dinucleoside

monophosphates. Therefore, we decided to use an additional internal standard for the SPE and the hydrolysis steps. We chose a series of oligonucleotides of different size bearing the unnatural DNA nucleoside εdAdo. A known amount of oligo-εdAdo was added to the sample to analyze before SPE. The concentration of recovered εdAdo was determined in the final analysis by MS/MS detection with isotopic dilution. The recovery yield was calculated in each sample and applied to the photoproducts.

Design of an UHPLC-MS/MS assay with on-line SPE purification

Because of the strong matrix effect in urine, we felt necessary to improve the resolution of the chromatographic separation in order to better separate analytes from interfering peaks. We therefore used UHPLC rather than HPLC columns. This now widely applied technology (43, 44) also allows using larger flow rates and reducing the analysis times. We also wanted to further increase the purity of the sample prior to its introduction into the analytical column. In order to keep this step as short as possible and limit the risk of losing material, we used an on-line SPE approach (45, 46). In this technique, the analysis set-up consists of two independent chromatography systems. One harbors the injector and is fitted with a usually small chromatography column that acts as an on-line SPE column. The other chromatographic part contains the classical analytical column and the detector. These two liquid chromatography systems are connected through a 6-ways valve. Upon injection, the sample is introduced by the flow of the purification part into the on-line SPE column. The conditions are chosen to allow the elution of a maximum of impurities but not of the analytes. After this washing step, the valve commutes and the analytes are transferred to the analytical column by the flow of the analytical pump. On-line SPE is especially efficient if the stationary phases of the two columns are different. Therefore, we used C18 and mixed C18-PFP silica gel columns for SPE and analysis, respectively.

The on-line SPE step was optimized through three parameters. The first was the composition of the mobile phase. Because photoproducts of dinucleoside monophosphate are polar, we used an isocratic elution with a pure aqueous phase to prevent a too fast elution from the small SPE column. For the same reason, we increased the concentration of the buffer of the aqueous phase. Like in the first SPE step, we used TEAA as a volatile ion-pairing agent. In the classical HPLC-MS/MS assay, its concentration is kept below 5 mM to remain compatible with the electrospray ionization. In this on-line SPE step, it could be raised to 20 mM because the eluent does not enter the mass spectrometer. This high TEAA concentration provided better peak shapes and more reproducible retention times. Other important parameters are the flow rate and the time at which the 6-ways valve of the on-line SPE commutes from 'Load' to 'Inject'. These two parameters are linked because they define the amount of solvent used to carry the sample to the SPE column as well as the amount of eluent used for the washing step. Again, these parameters have to be finely tuned to ensure the most efficient cleaning of the sample without loss of analytes. After full optimization of all the parameters of the SPE and the analytical chromatography, we obtained a method greatly improved compared to the classical HPLC approach (**Erreur ! Source du renvoi introuvable.**) in terms of peak shape, duration of analysis, signal to noise ratio and reproducibility of the retention times. The chromatographic conditions provided sensitive and specific detection of TT CPD *c,s* and TT 64PP but also of TT Dewar and TT CPD *t,s*, the TT CPD *trans,syn* diastereoisomer. The latter photoproduct is produced in dinucleoside monophosphates but not in B-form DNA because of the specific orientation of thymine bases in the double-helix.

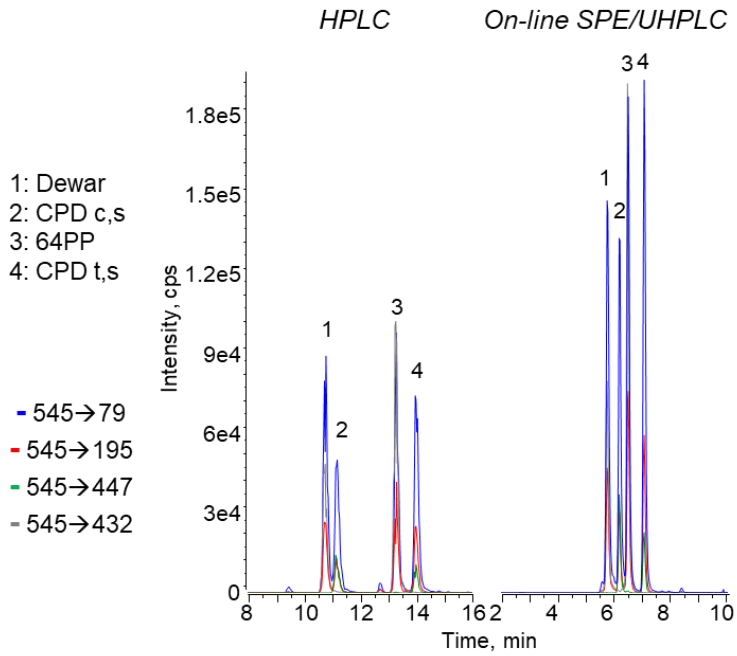

Figure 2: Comparison of the MS/MS detection of authentic TpT photoproducts (1 pmol injected) following either HPLC or on-line/UHPLC separation. The color of the chromatograms corresponds to the different fragmentation reactions monitored.

Evaluation of the performances of the method

Final design

The individual steps optimized above for the quantification TT CPD *c,s* and TT 64PP in biological samples were combined in a final protocol. First, oligo-εdAdo are added to the urine or culture medium samples. The sample is then deposited on top of a conditioned HRX-100 SPE column and washed with a buffer containing 15% MeOH. The elution is then performed with a 3/1 v/v mixture of MeOH and aqueous TEAA. After removal of the liquid phase, the sample residue is solubilized in a solution containing [M+12]-TpT photoproducts and [M+5]-εdAdo. The resulting solution is enzymatically hydrolyzed, filtered at 0.2 µm and analyzed by on-line SPE/UHPLC-MS/MS. It should be added that we used quality control samples in all sets of analyses to check the stability of the detection and of the recovery of the

analyte in the SPE step. A correction factor was applied that corresponded to the ratio between the concentration of εdAdo in each sample and the mean of that determined in the QC.

Calibration curves

Validation of the method was based on recommendations of the Food and Drug Administration (47) and the Scientific Working Group for Forensic Toxicology (48). In a first step, we validated the calibration curves. For this purpose, we injected on five different days triplicates of four different concentrations of standards, and a control. All vials contained the same amount of internal standard and were all prepared independently. All standards and internal standards used for the intra- and inter-day comparisons were taken from the same stock solutions. A calibration curve was determined with the most specific transition for each photoproduct, namely 545→447 for TT CPD *c,s* and 545→432 for TT 64PP. As shown on figure S7 in supplementary material, all values fell into the ± 15% range. Two exceptions were observed for the lowest concentration, 1 for TT CPD *c,s* in validation 1 and 1 for TT 64PP in validation 3. The reproducibility of the calibration curve is also shown by the variation coefficients (v.c.) that are 8.9 and 8.6 % at the lowest concentration for TT CPD *c,s* and TT 64PP, respectively. The corresponding values at the largest concentration are 3.7 and 4.0 %. An ANOVA analysis also showed the repeatability and reproducibility of the calibration curves (see Electronic Supplementary Material Table S2).

Analytical validation

We then validated the overall analytical procedure applied to both urine and culture medium from the initial SPE step to the final analysis with the oligo-εdAdo correction. A preliminary study was the determination of the recovery in series of quality control samples prepared in water. TEAA and all internal standards were added and purified by SPE on four consecutive days. Four samples were included in each series. Each series was analyzed independently. The

recovery value was slightly larger than 100 % and very reproducible as shown by value of v.c. below 10 % (Supplementary information Table S3). A similar protocol was used to validate the analysis in urine. On four consecutive days, we purified by SPE 200 µL of urine spiked with a solution of UV-exposed oligonucleotide (final concentration: 2.5 nM TT CPD *c,s* and 1.3 nM TT 64PP). The SPE-purified fraction was then enzymatically hydrolyzed and analyzed by on-line SPE/UHPLC-MS/MS. An ANOVA analysis was performed on the four series of five values associated with a Fisher test. Quantification of both TT CPD *c,s* and TT 64PP was validated since F values of 0.284 and 1.089 were obtained, respectively. They are below the critical F value of 3.056. The v.c. were 14.6 and 18.1 % TT CPD *c,s* and TT 64PP, respectively, while the recovery yield was 92 and 97% (Supplementary information Table S4). A similar work was performed in culture medium. The value of the Fisher test were 2.48 and 0.62 for TT CPD *c,s* and 64 PP, respectively (critical value: 3.24). The corresponding v.c. were 12 and 14 %. An additional parameter of the validation is the study of the carry-over. It was not observed in blank samples injected immediately after the most concentrated standard of the calibration curve.

Limits of detection and quantification

Other major points investigated were the limits of detection (LOD) and quantification (LOQ). For this purpose, we used the approach based on the calculation of the mean and standard deviation of the noise at the elution time of the analyte of interest. The LOD is mean + 3×SD and LOQ is mean + 10×SD (49, 50). The values reported in Table 1 show that, as previously observed with our initial HPLC-MS/MS assay (9, 42), the detection of TT 64PP is more sensitive than that of TT CPD *c,s*, by factor of 3, 5 and 8 in water, medium and urine, respectively. As a general trend, the sensitivity of the assay is 20 to 50 times better than in our previous assay (9). This is partly explained by the fact that we are presently using a more recent mass spectrometer, but also by the improvement of the chromatography. The LOD and LOQ

values also show that injection in culture medium rather than in water decreases the sensitivity by a factor 10 for TT CPD *c,s* and 6 for TT 64PP. The impact of SPE-purified urine is much stronger with attenuation of the response by factors of 60 and 25 for TT CPD *c,s* and 64PP, respectively. The difference in the effect of the two matrices can be explained by the larger amounts of solutes present in urine compared to medium, as shown by the UV chromatogram recorded during analysis (see Electronic Supplementary Material Fig. S8). It may be added that, as expected, the values of the LOD and LOQ were proportional to the amount of urine purified in the SPE step. Therefore, increasing the volume of urine to improve the overall sensitivity of the assay is not a suitable option. For this reason, we choose a compromise of the analysis of 100 or 200 µL urine fractions.

Table 1: Sensitivity of the detection of TT CPD *c,s* and TT 64PP in water, culture medium and urine. Reported data are values of limits of detection (LOD) and limits of quantification (LOQ) expressed in fmol for standards injected in solution in water, medium and SPE-purified urine. For the latter, 200 µL were purified by SPE, resuspended in 100 of TEAA and used for the preparation of the standards. In all cases, the injection volume was 50 µL.

fmol detected		water	medium	urine
TT CPD m/z 545 → 447	LOD	0.7	7.6	51
	LOQ	2.4	21	130
TT 64PP m/z 545 → 432	LOD	0.3	1.5	6.7
	LOQ	0.8	4.4	17

Robustness

We used 78 samples of human urine collected in the absence of significant exposure to UV to test the robustness of the assay. The SPE isolation protocol and the on-line/UHPLC-MS/MS

protocol was applied to 100 µL of each sample. The analyses sequence consisted in 6 series of injections each including a blank (water), 4 calibration solutions, a blank, 13 urine samples, a QC and a blank. Calibration solutions were also injected a 7th time at the end. A first observation was the lack of detection of the photoproducts in the analyzed urines, which were collected in winter, namely in the absence of significant exposure to solar UV. A few chromatograms exhibited tiny peaks for one the three transitions monitored for TT 64PP or TT CPS *c,s*, but never simultaneously the signals of the three expected ions. This result shows that no significant interferences are expected. Analysis of the intensity of the signal of the [M+12]-internal standards was a first evidence of the robustness of the assay (**Erreur ! Source du renvoi introuvable.**a). No drift in the value of the peak area was observed for [M+12]-TT CPD *c,s*. A slight trend to a decrease was observed for [M+12]-TT 64PP but the loss of signal was limited to approximately 10 %. Variations in the signal of internal standards were observed between samples but this was expected because it reflects differences in the matrix effect due to variation in the urine concentration. Another evidence of the robustness of the assay was obtained by the determination of calibration curves based on the area of the analytes peaks. In this sequence of analyses, the four solutions used for the determination of the calibration curves were injected 7 times. It was thus possible to evaluate the evolution of the sensitivity of the detection (**Erreur ! Source du renvoi introuvable.**b). As observed for internal standards, a visible but limited decrease in the sensitivity was observed for TT 64PP but not for TT CPD *c,s*. It should be emphasized that the use of internal standards compensates for these variations and insures the quantitative aspects of the results.

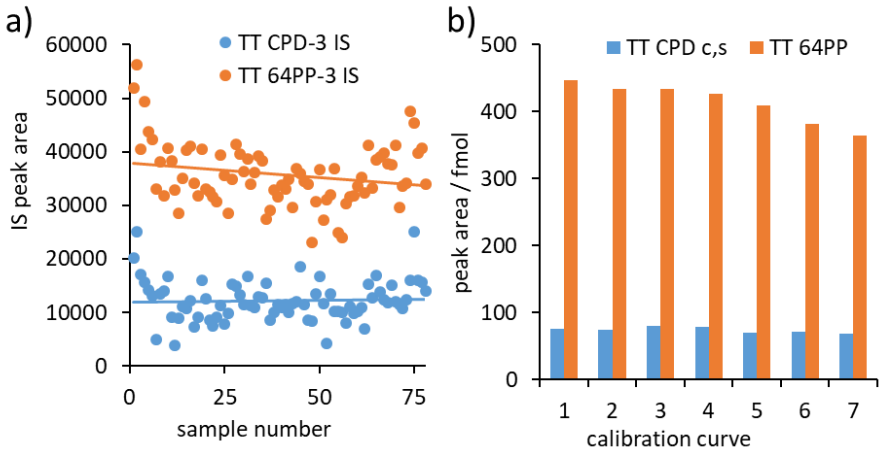

Figure 3: Robustness of the on-line SPE/UHPLC-MS/MS detection of TT CPD c,s and TT 64PP in a series of urine analyses; a) : value of the signal of internal standards (IS) in the urine samples and b) evolution of the sensitivity of the detection inferred from the repeated calibrations.

Biological validation

Fate of DNA photoproducts in HaCat cells

In a first protocol referred to as "cumul" (Scheme 2), HaCat cells were exposed to SSL in PBS and then replaced in fresh culture medium. After increasing period (0, 3, 24, 48, 72 and 96 h), the culture medium was collected and the cells isolated. The cellular pellet was divided in two parts, one for DNA extraction and the other for isolation of rep-oligos from the cytoplasmic fraction. The content in TT CPD *c,s* and TT 64PP was determined in the three sets of samples (**Erreur ! Source du renvoi introuvable.**a et b). The level of photoproduct in nuclear DNA, determined using an improved version of our previously designed HPLC-MS/MS assay (see Electronic Supplementary Material), continuously decreased during the investigated period, with less than 20% TT CPD remaining after 96 h. For TT CPD, statistically significant differences were observed between 0h and 72h ($p<0.01$) and 96 h ($p<0.001$), as well as between 2h and 72h ($p<0.05$) and 96 h ($p<0.01$). TT 64PP was much more efficiently repaired and not detected in DNA after 24h. The differences were statistically significant between 0h and 24,

48, 72 and 96h ($p<0.001$), as well as between 2h and all later time points ($p<0.05$). An opposite trend was observed for the culture medium with a constant increase in concentration of both photoproducts with increasing time. For CPD, differences reach statistical significance between 0h and 96h ($p<0.05$), 2h and 72h ($p<0.01$) and 2h and 96h ($p<0.01$). In the case of 64PP, the differences were statistically different between, 0h and 72h ($p<0.05$), 0h and 96 ($p<0.05$), 2h and 72h ($p<0.05$), and 2h and 96h ($p<0.05$). The difference between 0h and 48h was also statistically significant. ($p<0.05$). The concentration in the cytoplasmic extract exhibited a bell-shaped profile. The maximum value was obtained at 24h for both photoproducts and then slowly decreased. At this time point, the CPD concentration was significantly larger than that at 0h ($p<0.001$), 72h ($p<0.05$) and 96h ($p<0.01$). In the case of 64PP, the value at 0h was significantly lower than at 2h ($p<0.01$), 24h ($p<0.01$) and 48h ($p<0.01$), as well as larger at 24h than 96h ($p<0.01$), The decrease was slower for TT 64PP than TT CPD since the concentration at 96h represented 42 and 25% of that at 24h, respectively. These observations illustrate that upon repair, photoproducts contained in rep-oligos are released in the cytoplasm, in agreement with previous works (28). The synchronicity between the time-course level of photoproducts in DNA, cytoplasm and medium is a strong argument that the latter dimers are really related to repair and not to other mechanism such as cell death. In this case, release in the medium should occur at earlier time post-exposure.

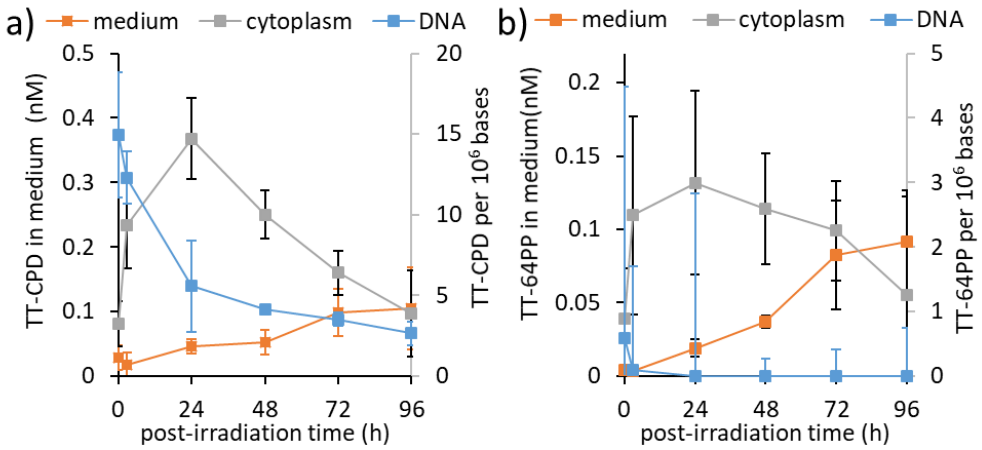

Figure 4: Evolution of the amount of photoproducts in DNA, cytoplasm and culture medium of HaCat cells exposed to simulated sunlight (0.5 MED). Cumul protocol was used up to 96h. a) TT CPD c,s b) TT 64PP. Concentrations in culture media and cytoplasmic extracts are expressed in nM. The levels in DNA are in photoproducts per million bases. Values are mean ± standard error (n=6). Statistical significance of the differences are presented in the "results and discussion" section.

In a second protocol called "renew" (Scheme 2), cells were placed in fresh culture medium after irradiation. The latter solution was collected after increasing time and replaced with fresh medium. At 96h, the cell pellet was collected and the content in photoproducts was determined in DNA and cytoplasm. We observed that, at 96 h, the cytoplasmic concentration was the same as in the "cumul" protocol (**Erreur ! Source du renvoi introuvable.**). Similarly, the amount of TT CPD c,s and 64PP released in the medium was similar in both type of experiments, when the values determined after each replacement of medium in the "renew" protocol were combined. We also observed that the extent of TT CPD *c,s* repair in DNA was very similar with both approaches. The repair yields were 82 and 87 % for the "renew" and "cumul" protocols, respectively. It may thus be concluded that changing the medium does not significantly modify the cellular response to UV-induced DNA damage. The possibility of using photoproducts in medium as biomarkers without disrupting cells for extracting DNA is thus biologically relevant.

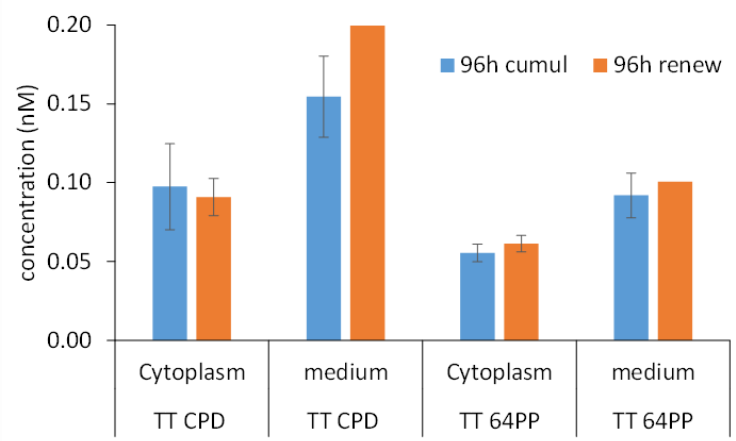

Figure 5: Concentration of photoproducts in cytoplasmic extracts and culture medium 96h after irradiation. "Cumul" corresponds to samples where the cells and culture medium were collected at the same time. "Renew" are for samples where the medium was collected and replaced by fresh medium at different times. In this case, the reported medium concentration is the sum of that in all individual collected media. The cytoplasm value is that in cells analyzed at 96 h, which is the last time point of the study. Values are mean ± standard error (n=6). No error is provided for the culture medium in the "renew" protocol because it is the sum of several values.

Release of rep-oligos from normal human skin explants

Human skin samples were freshly obtained from breast surgery on healthy patients. They were used to prepare a series of 1 cm punches cultured at the air/liquid interface on membranes placed in wells of culture plates. The explants were exposed to increasing doses of SSL (0.5, 1 and 2 MED). Like in the approach used in the "cumul" protocol applied to HaCat cells, the post-irradiation incubation was stopped after increasing time (1, 24 and 96h) and the medium was collected. Both TT CPD *c,s* and TT 64PP were detected after 24 and 96 h (**Erreur ! Source du renvoi introuvable.**). A constant increase with time was observed with statistically significant differences for 2 MED ($p<0.05$) between 1, 24 and 96h. The concentration in photoproducts in the medium was found to be dependent on the applied SSL dose, which was either 0.5, 1 or 2 MED. The concentration at 96h for 2 MED was statistically significantly larger than that at the

same time point for 1 MED ($p<0.05$) and 0.5 MED ($p<0.05$). The same was true for TT 64PP ($p<0.05$). No photoproduct was detected at 1 h, except a low amount of TT 64PP (0.02±0.004 nM) for 2 MED. These results are important for the validation of the biomarkers because they show that rep-oligos are not trapped in the complex multilayer structure of epidermis and upper dermis. The observation of their release in medium show that the rep-oligos can diffuse through layers of keratinocytes by para- or transcellular penetration. This is a requisite to their subsequent transfer in blood stream and ultimately excretion in urine.

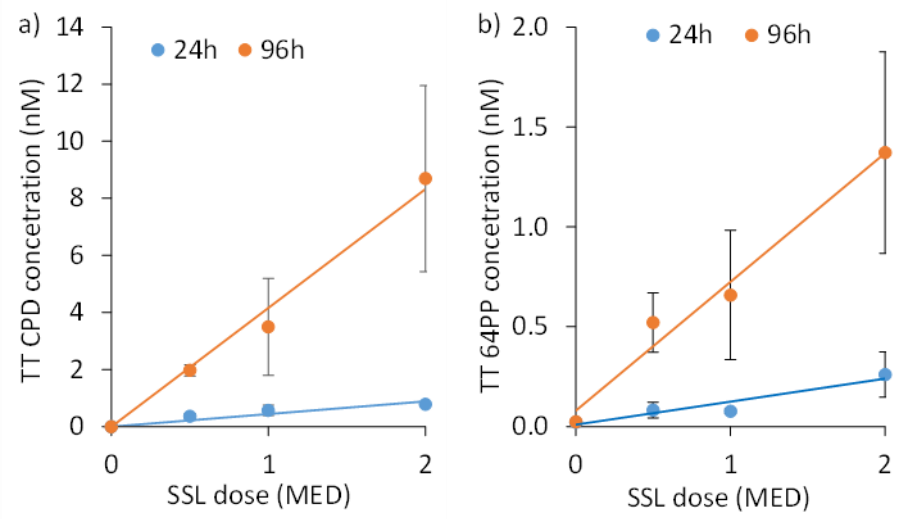

Figure 6: Increase in the concentration in a) TT CPD and b) TT 64PP in the medium of human explants collected either 24 or 96 h after exposure to increasing doses of SSL (0.5, 1 or 2 MED). Values are mean ± standard deviation (n=3). Statistical significance of the differences are presented in the "results and discussion" section.

Photoproducts in urine from sun-exposed volunteers

The last step of the biological validation of the use of photoproducts released in DNA repair products as biomarkers was a proof-of-concept in human samples. For this purpose, we analyzed urines from three volunteers submitted to recreational exposure during summer holidays. Isolation of rep-oligos by SPE followed by on-line SPE/UHPLC-MS/MS analysis unambiguously showed the presence of TT CPD *c,s* (**Erreur ! Source du renvoi introuvable.**).

Smaller signals were observed for TT 64PP (Supplementary information Fig. S9). It should be stressed that the peaks were strictly at the same retention times as the internal standards. The three expected ions were observed for TT CPD *c,s* in the same ratio as in standards. Equivalent observations were not possible for TT 64PP that were detected in too low amounts. The detection of TT CPD *c,s*, and with lesser confidence of TT 64PP, in urine is in line with results obtained by ^{32}P-poslabeling (25-27). Yet, we believe that our data are more quantitative. First, while the ^{32}P-post labeling assay targets only TT CPD *c,s* released as dinucleoside monophosphate, our method makes possible the isolation of the repair products of all sizes. In addition, the previous method included several steps for which the quantitative aspect was not controlled. Those included the UVC photoreversion of TT CPD *c,s* into TpT and the ^{32}P-labeling by polynucleotide kinase. Loss of material could take place in our protocol but it was compensated by the use of internal standards (isotopically labelled molecules and oligo-εdAdo).

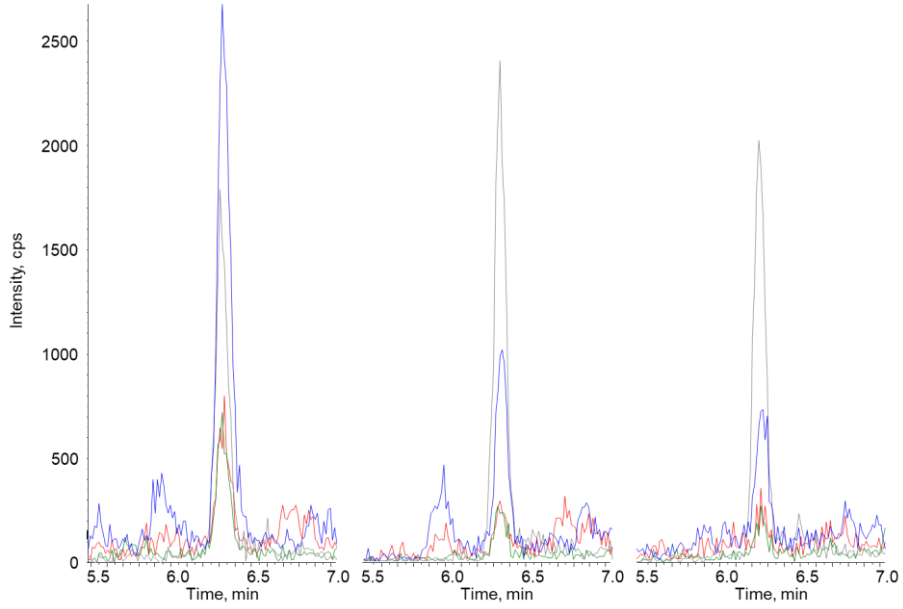

Figure 7: Detection of TT CPD c,*s* in urines collected from three volunteers after recreational exposure in summer. The color of the chromatograms corresponds to: - m/z 557→459 (internal standard), - m/z 545→79, - m/z 545→195 and - m/z 545→447.

CONCLUSION

The detection of DNA damage in urine is an attractive alternative to the quantification in nuclear DNA that requires collection of blood samples or biopsies (51). Several works have revealed the presence of DNA adducts in urine such as those of aflatoxin (52, 53), estrogen (54) or sulphur mustard (55, 56). All these adducts are unstable, spontaneously depurinate and are excreted from cells. The nucleoside 8-oxo-7,8-hydro-2'-deoxyguanosine (8-oxodGuo) is also frequently quantified in biological fluids (57-59). The origin of this oxidative stress biomarker remains yet to be completely identified. It is most unlikely to result from DNA repair since 8-oxodGuo is removed by glycosylases under the form of a base and not a nucleoside. Detoxification of the nucleotide pool is a more probable origin. To the best of our knowledge, no method has been designed to target the DNA damage-bearing oligonucleotides released by the nucleotide excision repair pathway. This is what we undertook in the present work for the quantification of UV-induced pyrimidine dimers. The assay, based on SPE and UHPLC-MS/MS was successfully validated. It was also used to show the biological relevance of the underlying hypothesis. Experiments on cultured HaCat cells showed that, after formation in nuclear DNA, photoproducts are excised by repair, transferred into the cytoplasm and finally extracted in the culture medium. Similar work on human skin explants showed that a more complex and dense tissue does not prevent the release of repair products. Last, a small human investigation showed that pyrimidine dimers could be readily detected in urine following classical recreational exposure to sunlight. This novel approach will be useful for *in vitro* studies since it allows determining the extent of DNA damage without destructive extraction of nuclear DNA. This is a major advantage for expensive or complex skin models, or when several parameters have to be monitored by different techniques. Quantification in urine will also obviously receive many applications in human studies, for example in the investigation of the link between exposure and risk or for the optimization of photoprotection strategies. Another

application both in models and *in vivo* could be the direct assessment of the DNA repair capacities.

CONFLICT OF INTEREST

The authors declare that they have no conflict of interest.

REFERENCES

1. Huang AH, Chien AL. Photoaging: a review of current literature. Curr Dermatol Rep. 2020;9:22-9, https://doi.org/10.1007/s13671-020-00288-0.
2. Bernard JJ, Gallo RL, Krutmann J. Photoimmunology: how ultraviolet radiation affects the immune system. Nat Rev Immunol. 2019;19:688-701, https://doi.org/10.1038/s41577-019-0185-9.
3. Subhadarshani S, Athar M, Elmets CA. Photocarcinogenesis. Curr Dermatol Rep. 2020;9:189-99, https://doi.org/10.1007/s13671-020-00307-0.
4. Brash DE. UV signature mutations. Photochem Photobiol. 2015;91:15-26, https://doi.org/10.1111/php.12377.
5. Cadet J, Douki T. Formation of UV-induced DNA damage contributing to skin cancer development. Photochem Photobiol Sci. 2018;17:1816-41, https://doi.org/10.1039/c7pp00395a.
6. Deleeuw SM, Simons WIM, Vermeer BJ, Schothorst AA. Comparison of melanocytes and keratinocytes in ultraviolet-induced DNA-damage per minimum erythema dose sunlight - Applicability of ultraviolet action spectra for risk estimates. J Invest Dermatol. 1995;105:259-63, https://doi.org/10.1111/1523-1747.ep12318107.
7. Setlow RB. The wavelengths in sunlight effective in producing skin cancer: a theoretical analysis. Proc Natl Acad Sci U S A. 1974;71:3363-6, https://doi.org/10.1073/pnas.71.9.3363.
8. Young AR, Chadwick CA, Harrison GI, Nikaido O, Ramsden J, Potten CS. The similarity of action spectra for thymine dimers in human epidermis and erythema suggests that DNA is the chromophore for erythema. J Invest Dermatol. 1998;111:982-8, https://doi.org/10.1046/j.1523-1747.1998.00436.x.
9. Douki T. The variety of UV-induced pyrimidine dimeric photoproducts in DNA as shown by chromatographic quantification methods. Photochem Photobiol Sci. 2013;12:1286-302, https://doi.org/10.1039/C3PP25451H.
10. Douki T. Sunlight-induced DNA damage: molecular mechanisms and photoprotection strategies. In: Wondrak GT, editor. Skin Stress Response Pathways: Environmental Factors and Molecular Opportunities: Springer Int. Publish.; 2016. p. 49-77, https://doi.org/10.1007/978-3-319-43157-4_3.

11. Kielbassa C, Roza L, Epe B. Wavelength dependence of oxidative DNA damage induced by UV and visible light. Carcinogenesis. 1997;18:811-6, https://doi.org/10.1093/carcin/18.4.811.

12. Mouret S, Baudouin C, Charveron M, Favier A, Cadet J, Douki T. Cyclobutane pyrimidine dimers are predominant DNA lesions in whole human skin exposed to UVA radiation. Proc Natl Acad Sci USA. 2006;103:13765-70, https://doi.org/10.1073/pnas.0604213103.

13. Perdiz D, Grof P, Mezzina M, Nikaido O, Moustacchi E, Sage E. Distribution and repair of bipyrimidine photoproducts in solar UV-irradiated mammalian cells. Possible role of Dewar photoproducts in solar mutagenesis. J Biol Chem. 2000;275:26732-42, https://doi.org/10.1016/S0021-9258(19)61437-7.

14. Kobayashi N, Katsumi S, Imoto K, Nakagawa A, Miyagawa S, Furumura M, et al. Quantitation and visualization of ultraviolet-induced DNA damage using specific antibodies: Application to pigment cell biology. Pigment Cell Res. 2001;14:94-102, https://doi.org/10.1034/j.1600-0749.2001.140204.x.

15. Mitchell D, Brooks B. Antibodies and DNA Photoproducts: applications, milestones and reference guide. Photochem Photobiol. 2010;86:2-17, https://doi.org/10.1111/j.1751-1097.2009.00673.x.

16. Varghese AJ. Photochemistry of nucleic acids and their constituents. Photophysiology. 7. New-York: Academic Press; 1972. p. 207-74,

17. Douki T, Voituriez L, Cadet J. Measurement of pyrimidine(6-4) photoproducts in DNA by a mild acidic hydrolysis hplc fluorescence detection assay. Chem Res Toxicol. 1995;8:244-53, https://doi.org/10.1021/tx00044a010.

18. Bykov VJ, Kumar R, Forsti A, Hemminki K. Analysis of UV-induced DNA photoproducts by ^{32}P-postlabeleing. Carcinogenesis. 1995;16:113-8, https://doi.org/10.1093/carcin/16.1.113.

19. Bykov VJ, Sheehan JM, Hemminki K, Young AR. In situ repair of cyclobutane pyrimidine dimers and 6-4 photoproducts in human skin exposed to solar simulating radiation. J Invest Dermatol. 1999;112:326-631, https://doi.org/10.1046/j.1523-1747.1999.00523.x.

20. Shih BB, Farrar MD, Cooke MS, Osman J, Langton AK, Kift R, et al. Fractional sunburn threshold UVR Doses generate equivalent vitamin D and DNA damage in skin types I-VI but with epidermal DNA damage gradient correlated to skin darkness. J Invest Dermatol. 2018;138:2244-52, https://doi.org/10.1016/j.jid.2018.04.015.

21. Douki T, von Koschembahr A, Cadet J. Insight in DNA repair of UV-induced pyrimidine dimers by chromatographic methods. Photochem Photobiol. 2017;93:207-15, https://doi.org/10.1111/php.12685.

22. Zhang N, Deng W, Li Y, Ma Y, Liu Y, Li X, et al. Formic acid of ppm enhances LC-MS/MS detection of UV irradiation-induced DNA dimeric photoproducts. Anal Chem. 2020;92:1197-204, https://doi.org/10.1021/acs.analchem.9b04327.

23. Douki T, Cadet J. Individual determination of the yield of the main-UV induced dimeric pyrimidine photoproducts in DNA suggests a high mutagenicity of CC photolesions. Biochemistry. 2001;40:2495-501, https://doi.org/10.1021/bi0022543.

24. Douki T, Court M, Cadet J. Electrospray-mass spectrometry characterization and measurement of far-UV induced thymine photoproducts. J Photochem Photobiol B: Biol. 2000;54:145-54, https://doi.org/10.1016/S1011-1344(00)00009-9.

25. Kotova N, Hemminki K, Segerback D. Urinary thymidine dimer as a marker of total body burden of UV-inflicted DNA damage in humans. Cancer Epidemiol Biomarkers Prev. 2005;14:2868-72, https://doi.org/10.1158/1055-9965.EPI-05-0164.

26. Le Curieux F, Hemminki K. Cyclobutane thymidine dimers are present in human urine following sun exposure: Quantitation using P-32-postlabeling and high-performance liquid chromatography. J Invest Dermatol. 2001;117:263-8, https://doi.org/10.1046/j.1523-1747.2001.01416.x.

27. Petersen B, Wulf HC, Triguero-Mas M, Philipsen PA, Thieden E, Olsen P, et al. Sun and ski holidays improve vitamin D Status, but are associated with high levels of DNA damage. J Invest Dermatol. 2014;134:2806-13, https://doi.org/10.1038/jid.2014.223.

28. Hu J, Choi JH, Gaddameedhi S, Kemp MG, Reardon JT, Sancar A. Nucleotide excision repair in human cells: fate of the excised oligonucleotide carrying DNA damage in vivo. J Biol Chem. 2013;288:20918-26, https://doi.org/10.1074/jbc.M113.482257.

29. Adar S, Hu J, Lieb JD, Sancar A. Genome-wide kinetics of DNA excision repair in relation to chromatin state and mutagenesis. Proc Natl Acad Sci USA. 2016;113:E2124-33, https://doi.org/10.1073/pnas.1603388113.

30. Hu J, Adar S, Selby CP, Liebler DC, Sancar A. Genome-wide analysis of human global and transcription-coupled excision repair of UV damage at single-nucleotide resolution. Genes Dev. 2015;29:948-60, https://doi.org/10.1101/gad.261271.115.

31. Hu J, Adebali O, Adar S, Sancar A. Dynamic maps of UV damage formation and repair for the human genome. Proc Natl Acad Sci USA. 2017;114:6758-63, https://doi.org/10.1073/pnas.1706522114.

32. Song J, Kemp MG, Choi JH. Detection of the excised, damage-containing oligonucleotide products of nucleotide excision repair in human cells. Photochem Photobiol. 2017;93:192-8, https://doi.org/10.1111/php.12638.

33. Choi JH, Han S, Kemp MG. Detection of the small oligonucleotide products of nucleotide excision repair in UVB-irradiated human skin. DNA Repair. 2020;86:102766, https://doi.org/10.1016/j.dnarep.2019.102766.

34. Carpenter MA, Ginugu M, Khan S, Kemp MG. DNA containing cyclobutane pyrimidine dimers is released from UVB-irradiated keratinocytes in a caspase-dependent manner. J Invest Dermatol. 2022; in press, https://doi.org/10.1016/j.jid.2022.04.030.

35. Douki T, Odin F, Caillat S, Favier A, Cadet J. Predominance of the 1,N^2-propano 2 '-deoxyguanosine adduct among 4-hydroxy-2-nonenal-induced DNA lesions. Free Radic Biol Med. 2004;37:62-70, https://doi.org/10.1016/j.freeradbiomed.2004.04.013.

36. Courdavault S, Baudouin C, Sauvaigo S, Mouret S, Candéias S, Charveron M, et al. Unrepaired cyclobutane pyrimidine dimers do not prevent proliferation of UVB-irradiated cultured human fibroblasts. Photochem Photobiol. 2004;79:145-51, https://doi.org/10.1111/j.1751-1097.2004.tb00004.x.

37. Ravanat JL, Douki T, Duez P, Gremaud E, Herbert K, Hofer T, et al. Cellular background level of 8-oxo-7,8-dihydro-2'-deoxyguanosine: an isotope based method to evaluate artefactual oxidation of DNA during its extraction and subsequent work-up. Carcinogenesis. 2002;23:1911-8, https://doi.org/10.1093/carcin/23.11.1911.

38. Walker V, Mills GA. Solid-phase extraction in clinical biochemistry. Ann Clin Biochem. 2002;39:464-77, https://doi.org/10.1258/000456302320314476.

39. Hennion MC. Solid-phase extraction: method development, sorbents, and coupling with liquid chromatography. J Chromatogr A. 1999;856:3-54, https://doi.org/10.1016/s0021-9673(99)00832-8.

40. Ciccimaro E, Blair IA. Stable-isotope dilution LC-MS for quantitative biomarker analysis. Bioanalysis. 2010;2:311-41, https://doi.org/10.4155/bio.09.185.

41. Tretyakova N, Goggin M, Sangaraju D, Janis G. Quantitation of DNA adducts by stable isotope dilution mass spectrometry. Chem Res Toxicol. 2012;25:2007-35, https://doi.org/10.1021/tx3002548.

42. Douki T, Court M, Sauvaigo S, Odin F, Cadet J. Formation of the main UV-induced thymine dimeric lesions within isolated and cellular DNA as measured by high performance liquid chromatography-tandem mass spectrometry. J Biol Chem. 2000;275:11678-85, https://doi.org/10.1074/jbc.275.16.11678.

43. Neue UD, Kele M, Bunner B, Kromidas A, Dourdeville T, Mazzeo JR, et al. Ultra-performance liquid chromatography technology and applications. In: Grushka E, Grinberg N, editors. Advances in Chromatography. Advances in Chromatography. 48. Boca Raton: Crc Press-Taylor & Francis Group; 2010. p. 99-143,

44. Maldaner L, Jardim I. The state of art of ultra performance liquid chromatography. Quim Nova. 2009;32:214-22, https://doi.org/10.1590/s0100-40422009000100036.

45. Chen LG, Wang H, Zeng QL, Xu Y, Sun L, Xu HY, et al. On-line coupling of solid-phase extraction to liquid chromatography-a review. J Chromatogr Sci. 2009;47:614-23, https://doi.org/10.1093/chromsci/47.8.614.

46. Pyrzynska K, Pobozy E. On-line coupling of solid phase extraction sample processing with high-performance liquid chromatography. Crit Rev Anal Chem. 2002;32:227-43, https://doi.org/10.1080/10408340290765533.

47. U.S. Department of Health and Human Services FaDA. Bioanalytical method validation guidance for industry. 2018 2018.

48. Scientific Working Group for Forensic Toxicology (SWGTOX). Standard practices for method validation in forensic toxicology. J Anal Toxicol. 2013;37:452-74, https://doi.org/10.1093/jat/bkt054.

49. Shrivastava A, Gupta V. Methods for the determination of limit of detection and limit of quantitation of the analytical methods. Chron Young Sci. 2011;2:21, https://doi.org/10.4103/2229-5186.79345.

50. International conference on harmonisation of technical requirements for registration of pharmaceuticals for human use. Validation of analytical procedures: text and methodology. 2005.

51. Cooke MS, Hu CW, Chang YJ, Chao MR. Urinary DNA adductomics - A novel approach for exposomics. Environ Int. 2018;121:1033-8, https://doi.org/10.1016/j.envint.2018.10.041.

52. Groopman JD, Zhu JQ, Donahue PR, Pikul A, Zhang LS, Chen JS, et al. Molecular dosimetry of urinary aflatoxin-DNA adducts in people living in Guangxi Autonomous Region, People's Republic of China. Cancer Res. 1992;52:45-52,

53. Kensler TW, Chen JG, Egner PA, Fahey JW, Jacobson LP, Stephenson KK, et al. Effects of glucosinolate-rich broccoli sprouts on urinary levels of aflatoxin-DNA adducts and phenanthrene tetraols in a randomized clinical trial in He Zuo township, Qidong, People's Republic of China. Cancer Epidemiol Biomarkers Prev. 2005;14:2605-13, https://doi.org/10.1158/1055-9965.EPI-05-0368.

54. Gaikwad NW, Yang L, Weisenburger DD, Vose J, Beseler C, Rogan EG, et al. Urinary biomarkers suggest that estrogen-DNA adducts may play a role in the aetiology of non-Hodgkin lymphoma. Biomarkers. 2009;14:502-12, https://doi.org/10.3109/13547500903121715.

55. Zhang Y, Yue L, Nie Z, Chen J, Guo L, Wu B, et al. Simultaneous determination of four sulfur mustard-DNA adducts in rabbit urine after dermal exposure by isotope-dilution liquid chromatography-tandem mass spectrometry. J Chromatogr B Analyt Technol Biomed Life Sci. 2014;961:29-35, https://doi.org/10.1016/j.jchromb.2014.04.050.

56. Roser M, Beal D, Eldin C, Gudimard L, Caffin F, Gros-Desormeaux F, et al. Glutathione conjugates of the mercapturic acid pathway and guanine adduct as biomarkers of exposure to CEES, a sulfur mustard analog. Anal Bional Chem. 2021;413:1337–51, https://doi.org/10.1007/s00216-020-03096-4.

57. Henriksen T, Weimann A, Larsen EL, Poulsen HE. Quantification of 8-oxo-7,8-dihydro-2 '-deoxyguanosine and 8-oxo-7,8-di-hydro-guanosine concentrations in urine and plasma for estimating 24-h urinary output. Free Radic Biol Med. 2021;172:350-7, https://doi.org/10.1016/j.freeradbiomed.2021.06.014.

58. Gan W, Liu X-L, Yu T, Zou Y-G, Li T-T, Wang S, et al. Urinary 8-oxo-7,8-dihydroguanosine as a potential biomarker of aging. Front Aging Neurosci. 2018;10, https://doi.org/10.3389/fnagi.2018.00034.

59. Zanolin ME, Girardi P, Degan P, Rava M, Olivieri M, Di Gennaro G, et al. Measurement of a urinary marker (8-hydroxydeoxy-guanosine, 8-OHdG) of DNA oxidative stress in epidemiological surveys: a pilot study. Int J Biol Markers. 2015;30:E341-E5, https://doi.org/10.5301/jbm.5000129.

DNA photoproducts released by repair in biological fluids as biomarkers of the genotoxicity of UV radiation

Noémie Reynaud, Laura Belz, David Béal, Daniel Bacqueville, Hélène Duplan, Camille Géniès, Emmanuel Questel, Gwendal Josse, Thierry Douki

ELECTRONIC SUPPLEMENTARY MATERIAL

Optimization of the analytical protocol

Figure S1: Comparison of the elution of a 15-bases long oligonucleotide (sequence CAT CTT ACA TTT TAC) on three SPE columns packed with different solid phases. Values of 100, 200 and 500 refer to the mass (in mg) of solid phase. The total recovery was 2.4, 2.0 and 0.5 pmol on HRX-100 (Macherey-Nagel), HRX-200 (Macherey-Nagel) and C18-500 (Hypersep X30, Thermo Scientifc) columns, respectively

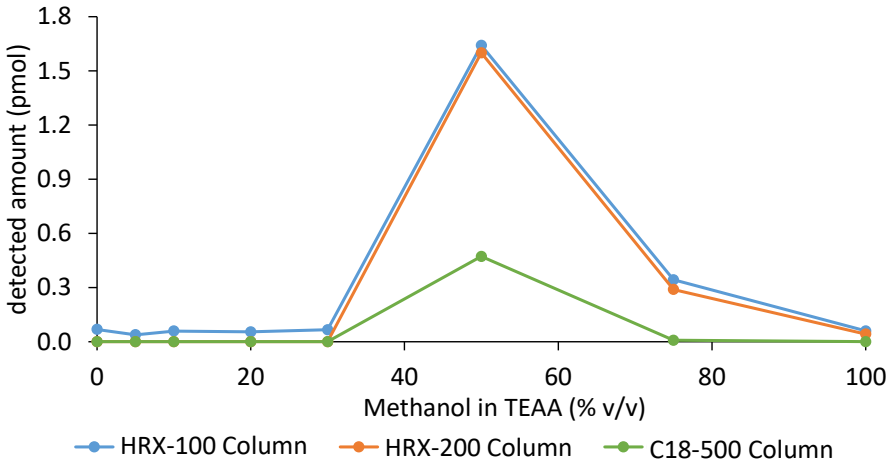

Figure S2: Optimization of the SPE for oligonucleotides in urine: a) comparison of the elution of a 5-mer and a 15-mer from HRX-100 columns with elution fractions containing 20 mM TEAA and increasing proportion of methanol (MeOH); b) Effect of the addition of TEAA into the urine sample and of the increase in the TEAA concentration of the elution solutions.

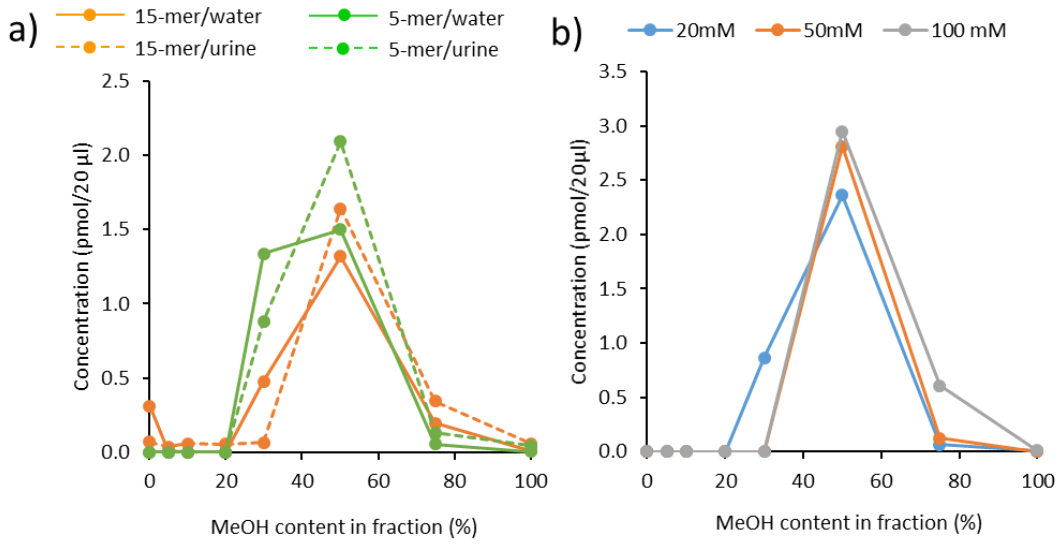

Figure S3: Synthesis of $^{13}C_{10}$,$^{15}N_2$-labelled TpT and its dimeric photoproducts.

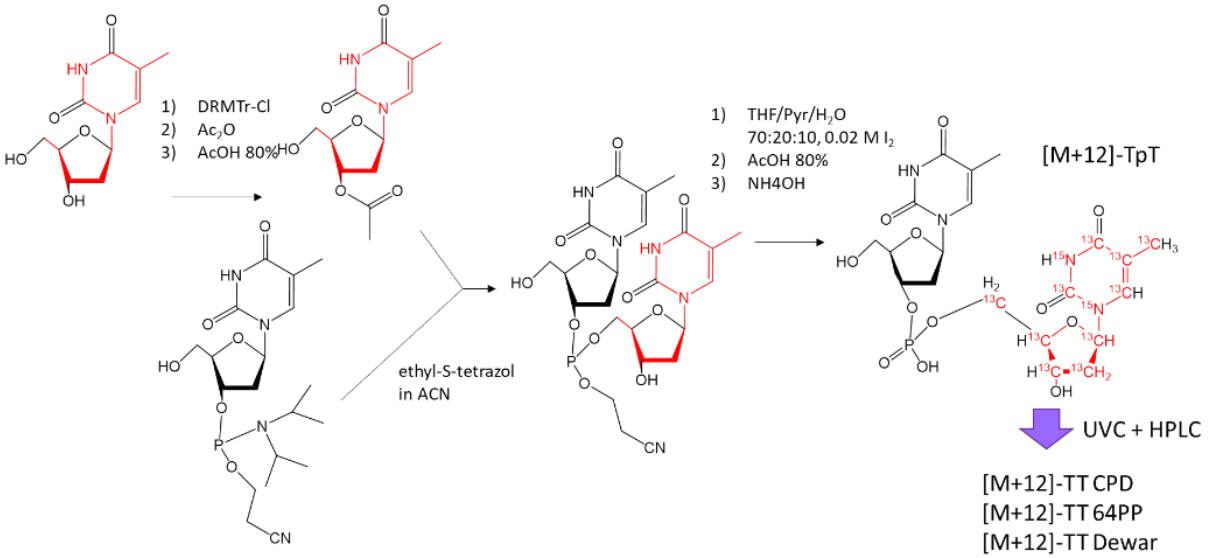

Figure S4: UHPLC analysis of the purified fraction containing $^{13}C_{10}$,$^{15}N_2$-labelled TpT. The UV detector was set between 220 and 320 nm. MS^1 detection was performed in negative ESI and the detection range was m/z = 200-800.

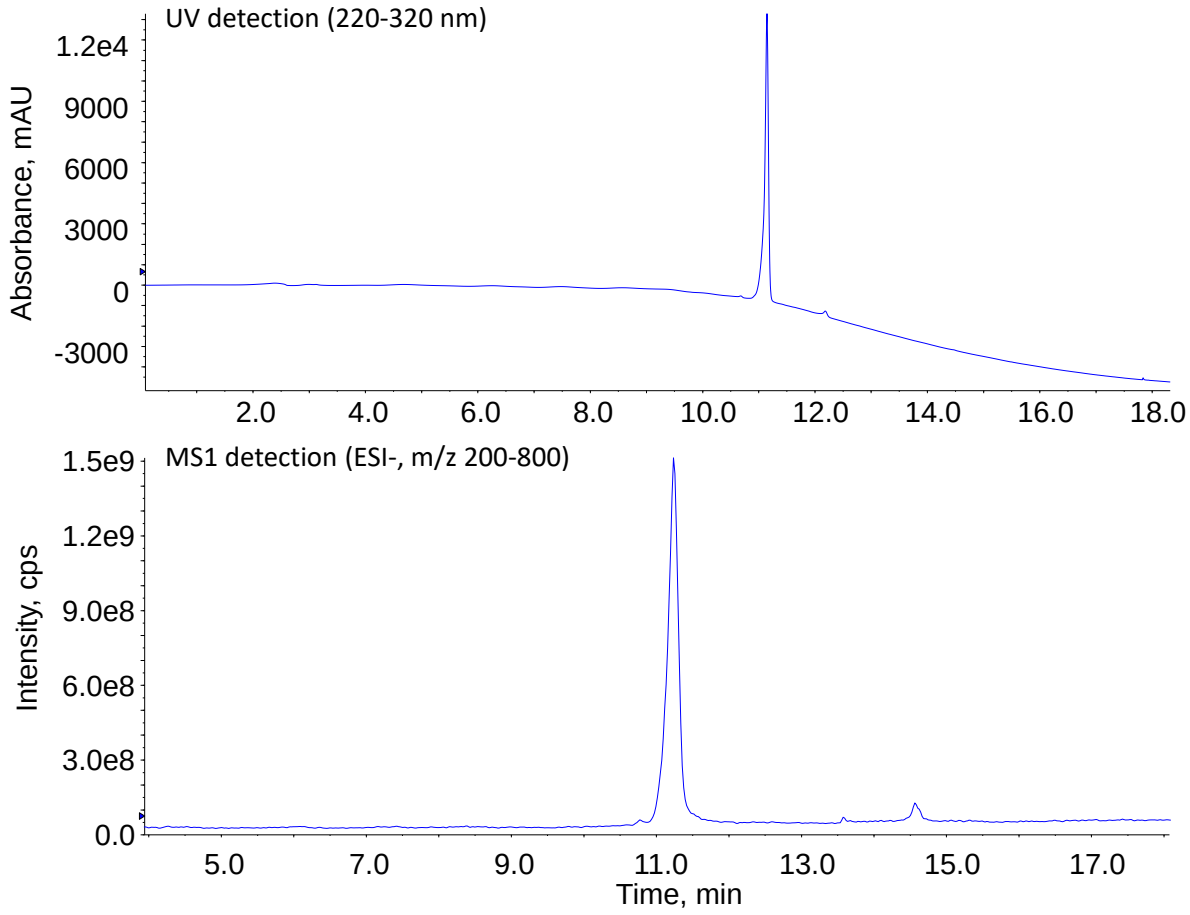

Figure S5: Mass spectrometry characterization of $^{13}C_{10}$,$^{15}N_2$-labelled TpT. MS^1 spectrum (upper trace) shows that the pseudo-molecular ion in the negative ESI mode is at m/z=557 as expected. The fragmentation mass spectrum recorded with a collision energy of -45 V (lower trace) exhibits fragments similar to those of unlabeled TpT. Those correspond to loss of bases and fragmentation of the phosphodiester bonds at various position (dR=deoxyribose, P=phosphate, Thy=thymine, Thd=thymidine).

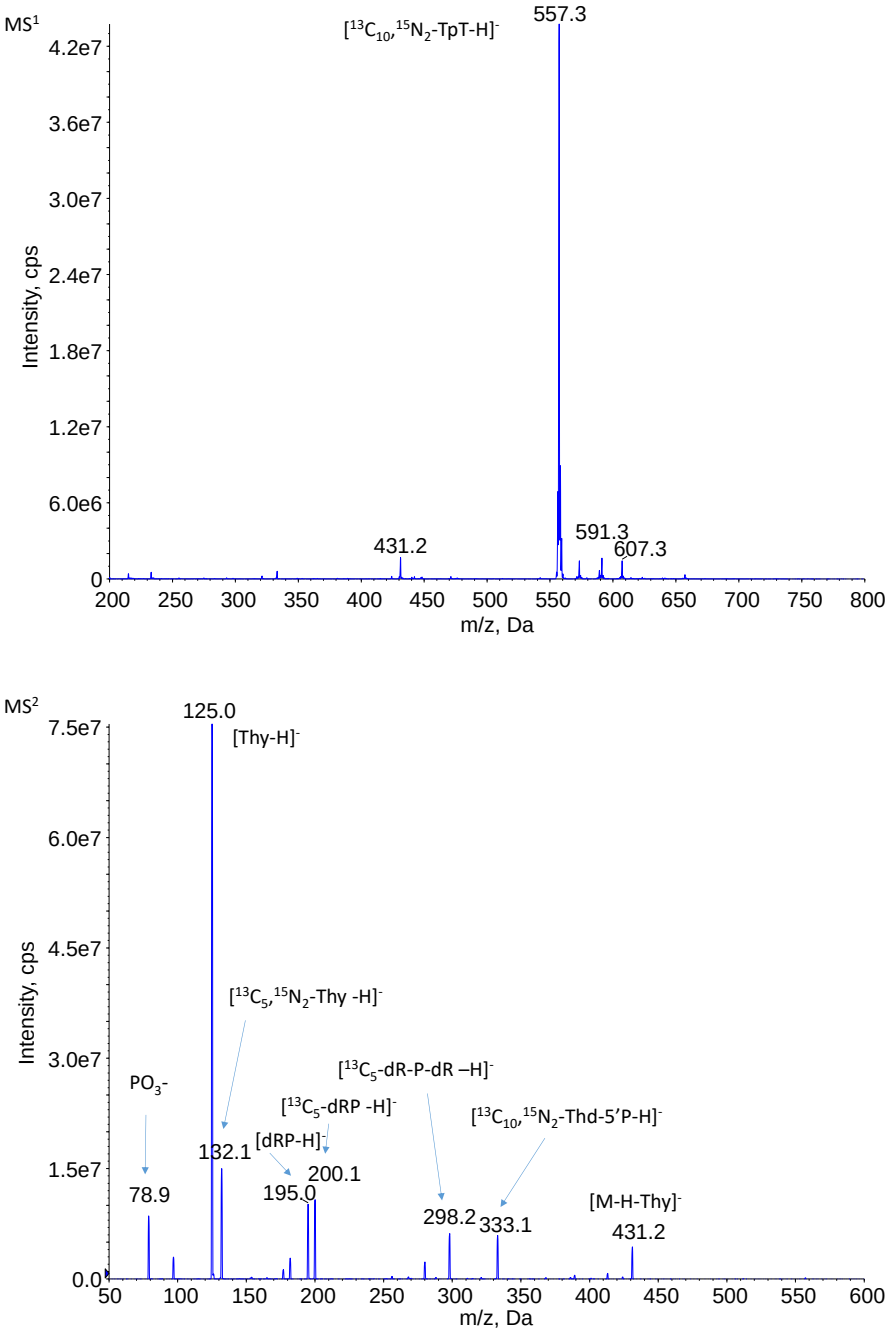

Figure S6: Fragmentation mass spectra of the [M+12]-TpT photoproducts (upper trace TT CDP *c,s*, lower trace TT 64PP) recorded with a collision energy of -45 V in negative ESI. Labeled fragments are those used for the MRM detection and correspond to those of unlabeled photoproducts (dR=deoxyribose, P=phosphate). The collision energy in the MRM mode is set à -110 V for m/z=79 to increase the intensity.

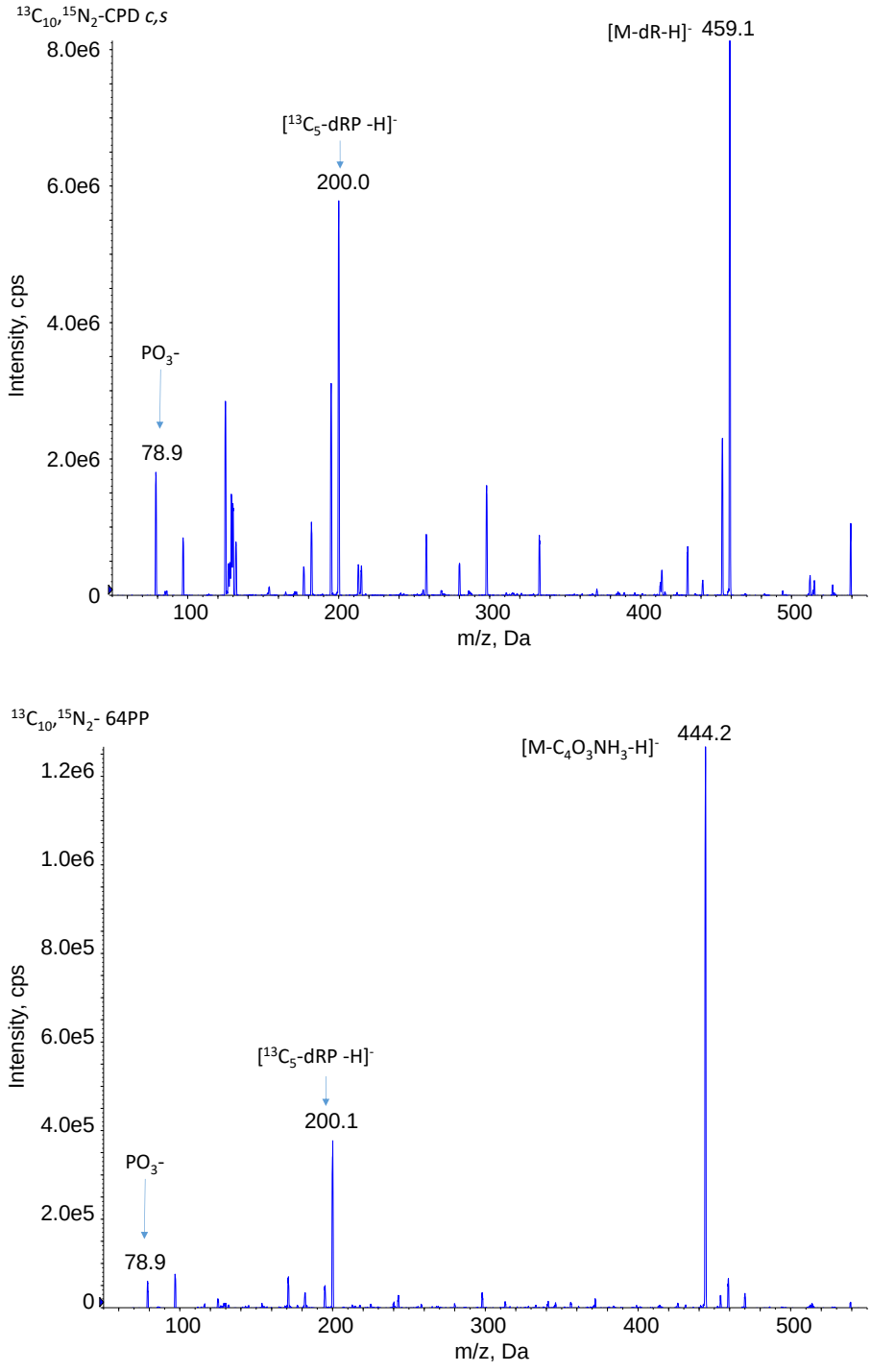

Table S1: Specific features of the analytes in the UHPLC-MS/MS assay. Rt is the retention time (in min). MRM are the fragmentation reactions. The first value is the m/z ratio of the pseudo-molecular ion ($[M-H]^-$ and $[M+H]^+$ in the negative and positive mode, respectively). The second value is the m/z ratio of the monitored fragments. The value in bracket is the collision energy. The internal standards (IS) are [M+12]-TpT photoproducts and [M+5]-εdAdo.

ID	Rt	MRM 1	MRM 2	MRM 3
TT CPD *c,s*	6.3	545.2→79.1 (-130)	545.2→195.1 (-47)	545.2→447.1 (-42)
TT 64PP	6.9	545.2→79.1 (-130)	545.2→195.1 (-47)	545.2→432.1 (-36)
TT CPD *t,s*	7.2	545.2→79.1 (-130)	545.2→195.1 (-47)	545.2→447.1 (-42)
TT Dewar	5.9	545.2→79.1 (-130)	545.2→195.1 (-47)	545.2→432.1 (-36)
TC CPD	4.6	531.2→79.0 (-130)	531.2→195.0 (-44)	531.2→433.1 (-40)
TC 64PP	6.6	530.2→79.0 (-128)	530.2→195.0 (-40)	
TC Dewar	6.3	530.2→79.0 (-128)	530.2→195.0 (-40)	
CC CPD	5.2	517.2→79.0 (-130)	517.2→195.0 (-40)	517.2→419.1 (-40)
TT CPD IS	6.3	557.2→79.1 (-130)	557.2→195.1 (-47)	557.2→459.1 (-42)
TT 64PP IS	6.7	557.2→79.1 (-130)	557.2→195.1 (-47)	557.2→444.1 (-36)
εdAdo	10.6	276.0→160.0 (19)		
εdAdo IS	10.6	281.0→165.0 (19)		

Evaluation of the performances of the method

Figure S7: Validation of the calibration of the on-line SPE/UHPLC-MS/MS assay for TT CPD *c,s* and TT 64PP. Urine samples (200 µL) from unexposed volunteers were purified by SPE. The obtained residue was resuspended in a TEAA solution and spiked with authentic standards. The final concentrations in photoproducts ranged between 5 and 45 nM. The injection volume was 50 µL. The red lines corresponds to the ± 15% interval.

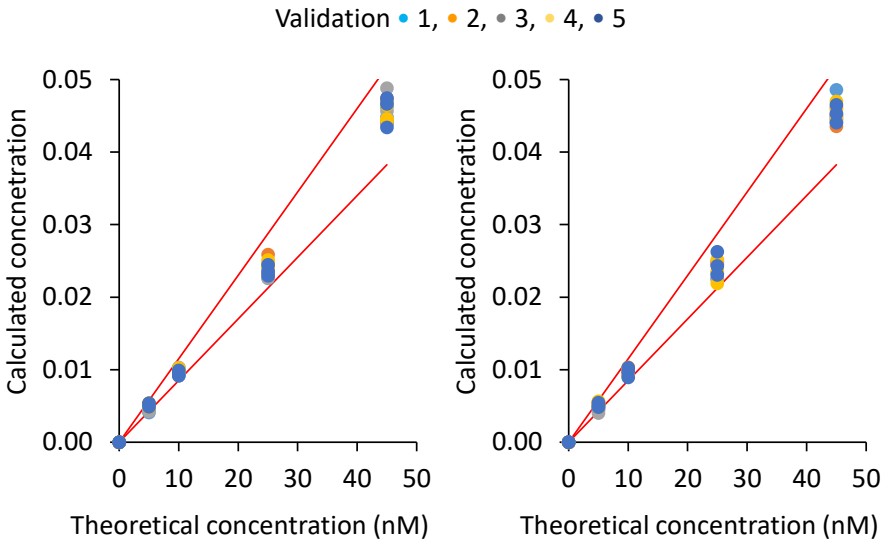

Table S2: validation of the calibration of the detection of TT CPD and TT 64PP in SPE-purified urine. Triplicates of three concentrations of standards were injected on four different days. The determined concentrations were used for an ANOVA analysis with a Fisher test. Under these conditions, the critical F value was 3.48. The table also reports the p values showing a lack of significant differences between the replicates.

	TT CPD		TT 64PP	
nM	F	*p*	F	*p*
5	1.73	0.22	2.34	0.13
10	0.68	0.62	0.23	0.92
25	1.37	0.31	1.47	0.28
45	0.19	0.94	0.25	0.90

Table S3: Validation of the method for quantification of TT photoproducts in quality control samples (QC). UV-irradiated oligonucleotide and oligo-εdAdo were added to 200 µL of an aqueous solution of TEAA. The samples were purified by SPE and further analyzed by on-line SPE/UHPLC-MS/MS after addition of isotopically labelled internal standards and enzymatic hydrolysis. The reported values are concentrations expressed in nM. Four series of 5 samples of QC were prepared and analyzed on separate days.

	TT CPD c,s		TT 64PP	
series #	Mean concentration	v.c. (%)	Mean concentration	v.c.(%)
1	2.93	11.2	1.77	9.2
2	2.67	1.6	1.53	2.9
3	2.94	5.2	1.73	0.8
4	2.76	4.3	1.53	3.5
combined	2.83	6.7	1.64	8.2
target	2.5		1.3	
recovery	113 %		123 %	

Table S4: Validation of the method for quantification of TT photoproducts in urine samples. Fractions of 200 µL of urine were spiked to 2.5 and 1.3 nM of TT CPD *c,s* and 64PP, respectively. All samples were analyzed by the complete method involving oligo-εdAdo and isotopically internal standards. Four series of 5 samples were analyzed on different days. The reported values are percentage of the target concentrations.

series #	Sample 1	Sample 2	Sample 3	Sample 4	Sample 5	mean	v.c. (%)
TT CPD c,s							
1	98	87	89	82	78	87	8.7
2	93	85	85	78	74	83	8.8
3	82	80	81	86	92	84	5.7
4	89	98	108	162	116	114	24.9
					combined	92	12
TT 64PP							
1	90	113	111	103	96	103	9.5
2	106	90	97	97	98	98	6.2
3	114	91	91	89	76	92	14.5
4	116	60	109	97	114	96	24.1
					combined	97	13.6

Figure S8: Comparison of the UV chromatogram (200-320 nm) recorded upon analysis of urine and cell culture medium.

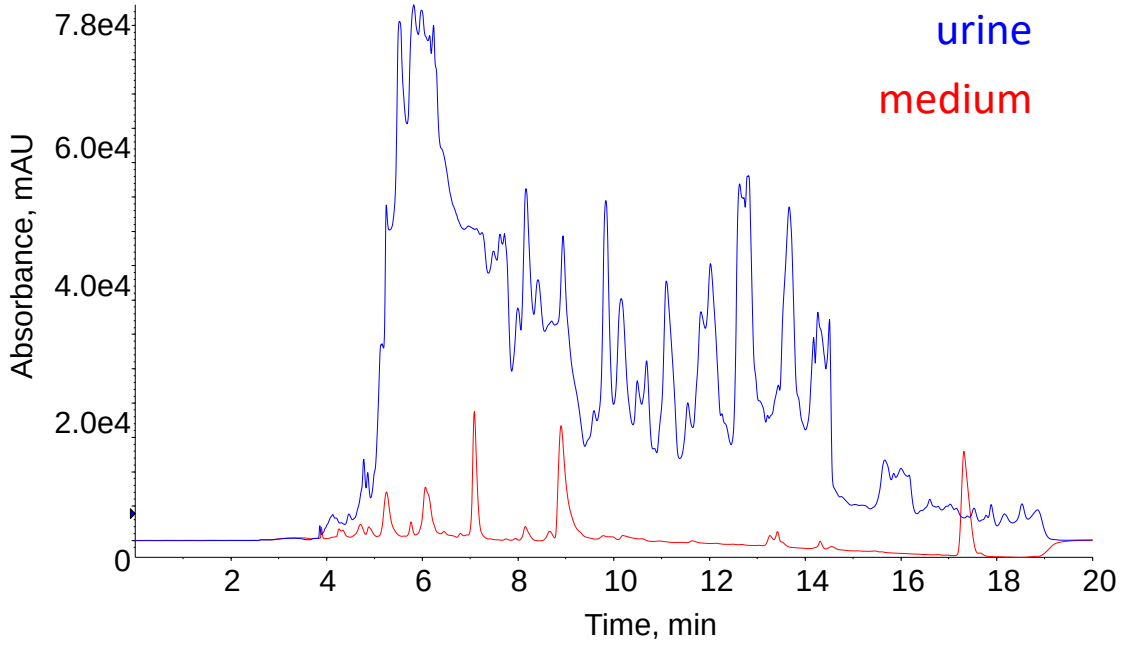

Biological validation

Figure S9: Detection of TT 64PP in urines collected from three volunteers after recreational exposure in summer. The color of the chromatograms corresponds to: m/z 557→444 (internal standard), m/z 545→79, m/z 545→195 and m/z 545→432.

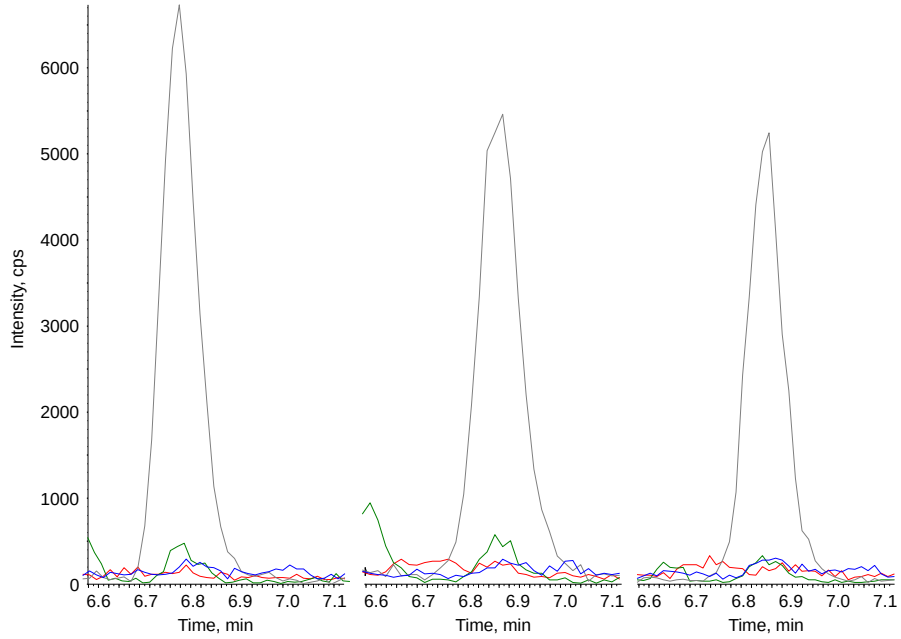

Extension of the assay to DNA

The performances of the on-line SPE/UHPLC-MS/MS assay for the quantification of TpT photoproducts in SPE-purified and hydrolyzed biological fluids prompted us to apply it to the analysis of photoproducts in DNA. In this case, the first SPE step is not necessary because DNA is isolated and purified during the extraction step from the cells or tissues of interest. We thus did not need to consider recovery yields and did not use the εdAdo normalization. Instead, we relied on the quantification of unmodified nucleosides to assess the amount of extracted and

injected DNA. This was done on-line by a diode array UV detector. Consequently, use of the presently developed approach is similar to its first step to our previous strategy (9). The main difference is that isotopically labeled internal standard have to be added. This was done by freeze-drying of the hydrolyzed samples and subsequent solubilization of the obtained residue in a solution containing [M+12]-TpT photoproducts. Quantification of each of the 4 TT photoproducts (CPD *c,s*, 64PP, Dewar and CPD *t,s*) was performed by internal calibration using equivalent MRM transition for each analyte and its [M+12]-labeled-derivative. Regarding the other photoproducts, it should be first reminded that cytosine-containing CPDs are detected under their deaminated form where uracil (U) replaces C. Therefore, the actual analytes are TU and UT CPD *c,s,* but TC and CT where kept in text for simplicity. The CC CPD *c,s* was not detected because we could not find satisfactory conditions to avoid its loss in the on-line SPE step. Isotopically labeled internal standards were not prepared for TC and CT photoproducts because of availability and cost of labeled molecules, and because of a more complex synthesis scheme requiring more protection steps than for [M+12]-TpT photoproducts. We thus used the TT internal standards for TC and CT photoproducts. We reasoned that, in contrast to complex matrices like urine where signal extinction can drastically vary during elution, use of internal standards in DNA are mostly useful for compensating fluctuations in the sensitivity of the mass spectrometer. MRM detection was based on specific fragmentations reactions (Table S1). All molecules yielded m/z=79 and 195 fragments, which correspond to fragmentation of the phosphodiester bonds. For the three quantified CPD *c,s*, a same additional fragmentation corresponding to the neutral loss of 98 (loss of a dehydrated 2-deoxyribose unit) is observed. The internal calibration of TC and CT CPD *c,s* was thus based on the 557→79, 557→195 and 557→459 transitions of [M+12] TT CPD *c,s*. No transition corresponding to the highly specific neutral loss of 113 observed for TT 64PP and Dewar is obtained for the related TC photoproducts. Therefore, we used only the 557→79 and 557→195 transitions of [M+12]-TT

64PP and Dewar for their internal calibration. The UHPLC gradient used was similar to that used for urine and culture medium with the exception that the first minute of elution on the on-line SPE column was isocratic and used 20 mM TEAA without ACN at a flow rate of 200 µL min^{-1}. All photoproducts could be detected separately (Figure S10). Some fragmentations were common to several photoproducts but those could be resolved based on their retention times.

Figure S10: On-line SPE/UHPLC-MS/MS detection of pyrimidine dimers (1.25 pmol of standard). The photoproducts and the monitored MRM transitions were: 1 TC CPD *c,s* (530→433); 2 CT CPD *c,s* (530→432), 3 TT Dewar (545→432), 4 TT CPD *c,s* (545→447), 5 TC Dewar (531→195), 6 TC 64PP (531→195), 7 TT 64PP (545→432), 8 TT CPD *t,s* (545→447)

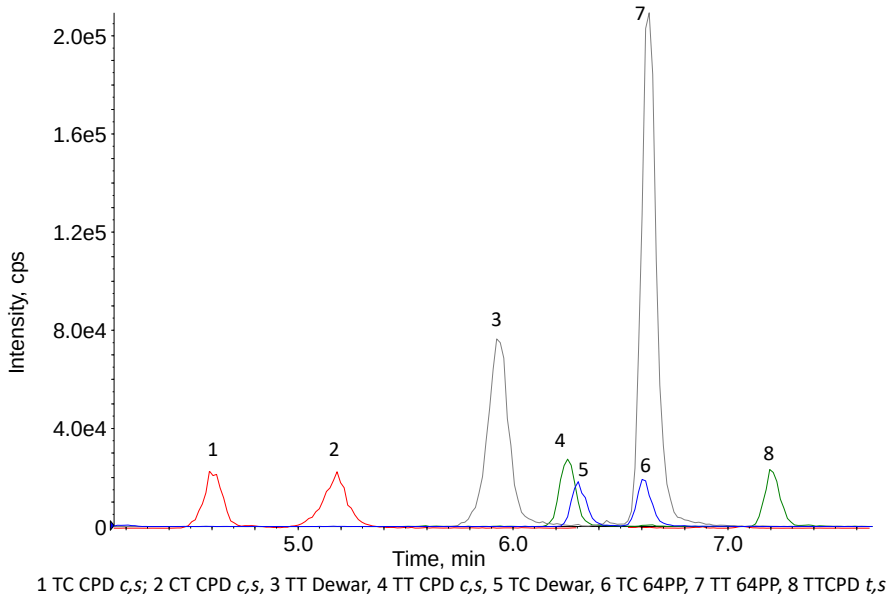

The calibration curves were determined by averaging the concentrations calculated for each MRM signal for each analyte. Exceptions were the TT 64PP and Dewar for which only the highly sensitive m/z 545→432 transition was used. The reproducibility and linearity of the calibration curves for TT, TC and CT photoproducts were then validated by injecting triplicates

of 4 different concentrations (5 to 45 nM) on 5 different days. We first estimated the deviation between the theoretical and the measured concentrations (Table S5). It was below 10% for all concentrations for TT CPD *c,s*, TT 64PP, TT Dewar, TT CPD *t,s*, and TC Dewar in the five series, with the exception of one sporadic series. In contrast, the deviation was above 10 % for TC and CT CPD at the lowest concentration when all results were combined. As a general trend, the deviation to the target concentrations was twice larger for TC and CT CPD than for the other photoproducts. These lesser quality of results is possibly explained by the use of TT CPD *c,s* as internal standard, which is eluting more than 1 min later than the corresponding TC photoprodutcs. The issue is not the same with the TC Dewar and 64PP that almost co-elute with their TT analogs. However, these larger deviations for some samples do not rule out the use of the method since they all remain below 15%. Regarding linearity, the slope of the curves comparing targeted and obtained calibration points differed from unity by less than 4 % for all photoproducts in all of the five individual series. All correlation coefficients were larger than 0.99. The lowest was 0.9923 for CT CPD and the largest 0.9995 for TT Dewar.

Table S5: Validation of the calibration curve for the quantification of photoproducts in DNA. Standards were in solution in water. The first values are variation coefficients (in %) determined upon validation of the calibration curve for photoproducts measured in DNA. Five series consisting of standards in 4 concentrations (plus a solution containing only the internal standard) injected three times were compared. The values in brackets are values of the Fisher tests obtained in an ANOVA analysis. Under the conditions of the experiment, the critical F value was 3.48. Conditions that exhibited statistically significant differences between replicated series of analyses are highlighted in bold.

Conc (µM)	TT CPD c,s	TT 64PP	TT Dewar	TT CPD *t,s*	TC CPD *c,s*	TC 64PP	TC Dewar	CT CPD *c,s*
0.005	8.5 (1.59)	8.9 (1.77)	6.6 (0.88)	7.5 (0.58)	**14.3 (16.7)**	8.1 (2.19)	7.5 (0.85)	**13.4 (8.05)**
0.01	5.2 (2.24)	4.7 (0.36)	3.5 (0.49)	3.6 (1.22)	9.6 (2.24)	5.0 (0.28)	5.1 (0.30)	8.7 (1.57)
0.025	4.1 (3.37)	5.1 (0.65)	**3.5 (5.49)**	**3.8 (3.69)**	7.4 (1.40)	4.2 (1.53)	5.4 (1.12)	8.9 (0.52)
0.045	3.7 (0.66)	4.0 (0.44)	3.7 (0.82)	4.2 (0.03)	5.8 (0.69)	4.0 (0.17)	3.6 (0.52)	5.2 (0.73)

In order to test the reproducibility and repeatability of the analysis in real samples, we exposed a 50 µg mL^{-1} (optical density of 1 at 260 nm) dialyzed solution of calf thymus DNA to a combination of UVB and UVA. The use of the two wavelength ranges aimed at increasing the content in Dewars (13, 60). In addition, the solution was prepared at low ionic strength in pure water in order to partially destabilize the DNA duplex and increase the yield in TT CPD *t,s* (61, 62). Another consequence of this irradiation protocol is that the TC and CT photoproducts are present in lower proportion than in stable B-DNA duplex (63). This could be seen as an advantage in the present study since the validation is thus made at low level for these photoproducts. The same stock solution of UV-exposed DNA was used in all analyses to avoid a source of variation linked to the irradiation step. Six series of five samples were analyzed for their content in photoproducts. The data (Table S6) showed that the repeatability was satisfactory with v.c. below 15% for TT 64PP, TT Dewar, TT CPD *t,s*, and TC 64PP. An

excellent performance was obtained for TT CPD *c,s* with intra v.c. below 3%. Poorer quality results were observed for TC CPD *c,s*, CT CPD *c,s* and TC Dewar. The data for the two former photoproducts are reminiscent of the observations made for the validation of the calibration curves. Similar observations were made regarding the reproducibility for which acceptable results (v.c. < 15%) were obtained for TT CPD *c,s*,, TT 64PP, TT Dewar, TC CPD *c,s*, and TC 64PP. For this criterium, large inter-day v.c. were obtained for TT CPD *t,s*, and TC Dewar. The final validation was made with an ANOVA analysis and a Fisher test. The reproducibility of the analyses was validated for all photoproducts except TT CPD *t,s* likely because the values for one of the series was below the five others.

Table S6: Reproducibility (inter for inter-day) and repeatability (intra for intra-day) of the on-line SPE/UHPLC-MS/MS quantification of photoproducts in isolated DNA exposed to UVA and UVB. Six series of 5 identical DNA samples were analyzed. The mean level of damage, the intra- and inter-series variation coefficients and the parameter of the Fisher test in the ANOVA were calculated.

	TT CPD *c,s*	TT 64PP	TT Dewar	TT CPD t,s	TC CPD c,s	TC 64PP	TC Dewar	CT CPD c,s
Level*	113±0. 5	3.3±0.1	4.8±0.1	8.4±0.3	10.6±0.3	14.5±0.3	6.0±0.2	10.6±0.3
v.c. intra min (%)	1.2	7.9	2.5	3.1	5.3	7.9	7.8	3.2
v.c. intra max (%)	2.9	11.2	11.0	9.6	23.7	11.2	25.4	17.7
v.c.. inter (%)	2.2	10.1	8.9	16.1	13.7	10.4	19.6	13.0
F†	2.5	1.9	2.0	28.0	0.8	1.9	0.5	1.4

* mean value for the 30 samples expressed in photoproducts per million bases (± SEM)

† the critical F value was 2.62 under the test conditions.

REFERENCES

1. Huang AH, Chien AL. Photoaging: a review of current literature. Curr Dermatol Rep. 2020;9:22-9, https://doi.org/10.1007/s13671-020-00288-0.

2. Bernard JJ, Gallo RL, Krutmann J. Photoimmunology: how ultraviolet radiation affects the immune system. Nat Rev Immunol. 2019;19:688-701, https://doi.org/10.1038/s41577-019-0185-9.

3. Subhadarshani S, Athar M, Elmets CA. Photocarcinogenesis. Curr Dermatol Rep. 2020;9:189-99, https://doi.org/10.1007/s13671-020-00307-0.

4. Brash DE. UV signature mutations. Photochem Photobiol. 2015;91:15-26, https://doi.org/10.1111/php.12377.

5. Cadet J, Douki T. Formation of UV-induced DNA damage contributing to skin cancer development. Photochem Photobiol Sci. 2018;17:1816-41, https://doi.org/10.1039/c7pp00395a.

6. Deleeuw SM, Simons WIM, Vermeer BJ, Schothorst AA. Comparison of melanocytes and keratinocytes in ultraviolet-induced DNA-damage per minimum erythema dose sunlight - Applicability of ultraviolet action spectra for risk estimates. J Invest Dermatol. 1995;105:259-63, https://doi.org/10.1111/1523-1747.ep12318107.

7. Setlow RB. The wavelengths in sunlight effective in producing skin cancer: a theoretical analysis. Proc Natl Acad Sci U S A. 1974;71:3363-6, https://doi.org/10.1073/pnas.71.9.3363.

8. Young AR, Chadwick CA, Harrison GI, Nikaido O, Ramsden J, Potten CS. The similarity of action spectra for thymine dimers in human epidermis and erythema suggests that DNA is the chromophore for erythema. J Invest Dermatol. 1998;111:982-8, https://doi.org/10.1046/j.1523-1747.1998.00436.x.

9. Douki T. The variety of UV-induced pyrimidine dimeric photoproducts in DNA as shown by chromatographic quantification methods. Photochem Photobiol Sci. 2013;12:1286-302, https://doi.org/10.1039/C3PP25451H.

10. Douki T. Sunlight-induced DNA damage: molecular mechanisms and photoprotection strategies. In: Wondrak GT, editor. Skin Stress Response Pathways: Environmental Factors and Molecular Opportunities: Springer Int. Publish.; 2016. p. 49-77,

11. Kielbassa C, Roza L, Epe B. Wavelength dependence of oxidative DNA damage induced by UV and visible light. Carcinogenesis. 1997;18:811-6, https://doi.org/10.1093/carcin/18.4.811.

12. Mouret S, Baudouin C, Charveron M, Favier A, Cadet J, Douki T. Cyclobutane pyrimidine dimers are predominant DNA lesions in whole human skin exposed to UVA radiation. Proc Natl Acad Sci USA. 2006;103:13765-70, https://doi.org/10.1073/pnas.0604213103.

13. Perdiz D, Grof P, Mezzina M, Nikaido O, Moustacchi E, Sage E. Distribution and repair of bipyrimidine photoproducts in solar UV-irradiated mammalian cells. Possible role of Dewar photoproducts in solar mutagenesis. J Biol Chem. 2000;275:26732-42, https://doi.org/10.1016/S0021-9258(19)61437-7.

14. Kobayashi N, Katsumi S, Imoto K, Nakagawa A, Miyagawa S, Furumura M, et al. Quantitation and visualization of ultraviolet-induced DNA damage using specific antibodies: Application to pigment cell biology. Pigment Cell Res. 2001;14:94-102, https://doi.org/10.1034/j.1600-0749.2001.140204.x.

15. Mitchell D, Brooks B. Antibodies and DNA Photoproducts: applications, milestones and reference guide. Photochem Photobiol. 2010;86:2-17, https://doi.org/10.1111/j.1751-1097.2009.00673.x.

16. Varghese AJ. Photochemistry of nucleic acids and their constituents. Photophysiology. 7. New-York: Academic Press; 1972. p. 207-74,

17. Douki T, Voituriez L, Cadet J. Measurement of pyrimidine(6-4) photoproducts in DNA by a mild acidic hydrolysis hplc fluorescence detection assay. Chem Res Toxicol. 1995;8:244-53, https://doi.org/10.1021/tx00044a010.

18. Bykov VJ, Kumar R, Forsti A, Hemminki K. Analysis of UV-induced DNA photoproducts by ^{32}P-postlabeleing. Carcinogenesis. 1995;16:113-8, https://doi.org/10.1093/carcin/16.1.113.

19. Bykov VJ, Sheehan JM, Hemminki K, Young AR. In situ repair of cyclobutane pyrimidine dimers and 6-4 photoproducts in human skin exposed to solar simulating radiation. J Invest Dermatol. 1999;112:326-631, https://doi.org/10.1046/j.1523-1747.1999.00523.x.

20. Shih BB, Farrar MD, Cooke MS, Osman J, Langton AK, Kift R, et al. Fractional sunburn threshold UVR Doses generate equivalent vitamin D and DNA damage in skin types I-VI but with epidermal DNA damage gradient correlated to skin darkness. J Invest Dermatol. 2018;138:2244-52, https://doi.org/10.1016/j.jid.2018.04.015.

21. Douki T, von Koschembahr A, Cadet J. Insight in DNA repair of UV-induced pyrimidine dimers by chromatographic methods. Photochem Photobiol. 2017;93:207-15, https://doi.org/10.1111/php.12685.

22. Zhang N, Deng W, Li Y, Ma Y, Liu Y, Li X, et al. Formic acid of ppm enhances LC-MS/MS detection of UV irradiation-induced DNA dimeric photoproducts. Anal Chem. 2020;92:1197-204, https://doi.org/10.1021/acs.analchem.9b04327.

23. Douki T, Cadet J. Individual determination of the yield of the main-UV induced dimeric pyrimidine photoproducts in DNA suggests a high mutagenicity of CC photolesions. Biochemistry. 2001;40:2495-501, https://doi.org/10.1021/bi0022543.

24. Douki T, Court M, Cadet J. Electrospray-mass spectrometry characterization and measurement of far-UV induced thymine photoproducts. J Photochem Photobiol B: Biol. 2000;54:145-54, https://doi.org/10.1016/S1011-1344(00)00009-9.

25. Kotova N, Hemminki K, Segerback D. Urinary thymidine dimer as a marker of total body burden of UV-inflicted DNA damage in humans. Cancer Epidemiol Biomarkers Prev. 2005;14:2868-72, https://doi.org/10.1158/1055-9965.EPI-05-0164.

26. Le Curieux F, Hemminki K. Cyclobutane thymidine dimers are present in human urine following sun exposure: Quantitation using P-32-postlabeling and high-performance liquid chromatography. J Invest Dermatol. 2001;117:263-8, https://doi.org/10.1046/j.1523-1747.2001.01416.x.

27. Petersen B, Wulf HC, Triguero-Mas M, Philipsen PA, Thieden E, Olsen P, et al. Sun and ski holidays improve vitamin D Status, but are associated with high levels of DNA damage. J Invest Dermatol. 2014;134:2806-13, https://doi.org/10.1038/jid.2014.223.

28. Hu J, Choi JH, Gaddameedhi S, Kemp MG, Reardon JT, Sancar A. Nucleotide excision repair in human cells: fate of the excised oligonucleotide carrying DNA damage in vivo. J Biol Chem. 2013;288:20918-26, https://doi.org/10.1074/jbc.M113.482257.

29. Adar S, Hu J, Lieb JD, Sancar A. Genome-wide kinetics of DNA excision repair in relation to chromatin state and mutagenesis. Proc Natl Acad Sci USA. 2016;113:E2124-33, https://doi.org/10.1073/pnas.1603388113.

30. Hu J, Adar S, Selby CP, Liebler DC, Sancar A. Genome-wide analysis of human global and transcription-coupled excision repair of UV damage at single-nucleotide resolution. Genes Dev. 2015;29:948-60, https://doi.org/10.1101/gad.261271.115.

31. Hu J, Adebali O, Adar S, Sancar A. Dynamic maps of UV damage formation and repair for the human genome. Proc Natl Acad Sci USA. 2017;114:6758-63, https://doi.org/10.1073/pnas.1706522114.

32. Song J, Kemp MG, Choi JH. Detection of the excised, damage-containing oligonucleotide products of nucleotide excision repair in human cells. Photochem Photobiol. 2017;93:192-8, https://doi.org/10.1111/php.12638.

33. Choi JH, Han S, Kemp MG. Detection of the small oligonucleotide products of nucleotide excision repair in UVB-irradiated human skin. DNA Repair. 2020;86:102766, https://doi.org/10.1016/j.dnarep.2019.102766.

34. Carpenter MA, Ginugu M, Khan S, Kemp MG. DNA containing cyclobutane pyrimidine dimers is released from UVB-irradiated keratinocytes in a caspase-dependent manner. J Invest Dermatol. 2022;in press, https://doi.org/10.1016/j.jid.2022.04.030.

35. Douki T, Odin F, Caillat S, Favier A, Cadet J. Predominance of the 1,N^2-propano 2 '-deoxyguanosine adduct among 4-hydroxy-2-nonenal-induced DNA lesions. Free Radic Biol Med. 2004;37:62-70, https://doi.org/http://dx.doi.org/10.1016/j.freeradbiomed.2004.04.013.

36. Courdavault S, Baudouin C, Sauvaigo S, Mouret S, Candéias S, Charveron M, et al. Unrepaired cyclobutane pyrimidine dimers do not prevent proliferation of UVB-irradiated cultured human fibroblasts. Photochem Photobiol. 2004;79:145-51, https://doi.org/10.1111/j.1751-1097.2004.tb00004.x.

37. Ravanat JL, Douki T, Duez P, Gremaud E, Herbert K, Hofer T, et al. Cellular background level of 8-oxo-7,8-dihydro-2'-deoxyguanosine: an isotope based method to evaluate artefactual oxidation of DNA during its extraction and subsequent work-up. Carcinogenesis. 2002;23:1911-8, https://doi.org/10.1093/carcin/23.11.1911.

38. Walker V, Mills GA. Solid-phase extraction in clinical biochemistry. Ann Clin Biochem. 2002;39:464-77, https://doi.org/10.1258/000456302320314476.

39. Hennion MC. Solid-phase extraction: method development, sorbents, and coupling with liquid chromatography. J Chromatogr A. 1999;856:3-54, https://doi.org/10.1016/s0021-9673(99)00832-8.

40. Ciccimaro E, Blair IA. Stable-isotope dilution LC-MS for quantitative biomarker analysis. Bioanalysis. 2010;2:311-41, https://doi.org/10.4155/bio.09.185.

41. Tretyakova N, Goggin M, Sangaraju D, Janis G. Quantitation of DNA adducts by stable isotope dilution mass spectrometry. Chem Res Toxicol. 2012;25:2007-35, https://doi.org/10.1021/tx3002548.

42. Douki T, Court M, Sauvaigo S, Odin F, Cadet J. Formation of the main UV-induced thymine dimeric lesions within isolated and cellular DNA as measured by high performance liquid chromatography-tandem mass spectrometry. J Biol Chem. 2000;275:11678-85, https://doi.org/10.1074/jbc.275.16.11678.

43. Neue UD, Kele M, Bunner B, Kromidas A, Dourdeville T, Mazzeo JR, et al. Ultra-performance liquid chromatography technology and applications. In: Grushka E, Grinberg N, editors. Advances in Chromatography. Advances in Chromatography. 48. Boca Raton: Crc Press-Taylor & Francis Group; 2010. p. 99-143,

44. Maldaner L, Jardim I. The state of art of ultra performance liquid chromatography. Quim Nova. 2009;32:214-22, https://doi.org/10.1590/s0100-40422009000100036.

45. Chen LG, Wang H, Zeng QL, Xu Y, Sun L, Xu HY, et al. On-line coupling of solid-phase extraction to liquid chromatography-a review. J Chromatogr Sci. 2009;47:614-23, https://doi.org/10.1093/chromsci/47.8.614.

46. Pyrzynska K, Pobozy E. On-line coupling of solid phase extraction sample processing with high-performance liquid chromatography. Crit Rev Anal Chem. 2002;32:227-43, https://doi.org/10.1080/10408340290765533.

47. U.S. Department of Health and Human Services FaDA. Bioanalytical method validation guidance for industry. 2018 2018.

48. (SWGTOX) SWGfFT. Standard practices for method validation in forensic toxicology. J Anal Toxicol. 2013;37:452-74, https://doi.org/10.1093/jat/bkt054.

49. Shrivastava A, Gupta V. Methods for the determination of limit of detection and limit of quantitation of the analytical methods. Chron Young Sci. 2011;2:21, https://doi.org/10.4103/2229-5186.79345.

50. Use ICOHOTRFROPFH. Validation of analytical procedures: text and methodology. 2005.

51. Cooke MS, Hu CW, Chang YJ, Chao MR. Urinary DNA adductomics - A novel approach for exposomics. Environ Int. 2018;121:1033-8, https://doi.org/10.1016/j.envint.2018.10.041.

52. Groopman JD, Zhu JQ, Donahue PR, Pikul A, Zhang LS, Chen JS, et al. Molecular dosimetry of urinary aflatoxin-DNA adducts in people living in Guangxi Autonomous Region, People's Republic of China. Cancer Res. 1992;52:45-52,

53. Kensler TW, Chen JG, Egner PA, Fahey JW, Jacobson LP, Stephenson KK, et al. Effects of glucosinolate-rich broccoli sprouts on urinary levels of aflatoxin-DNA adducts and phenanthrene tetraols in a randomized clinical trial in He Zuo township, Qidong, People's Republic of China. Cancer Epidemiol Biomarkers Prev. 2005;14:2605-13, https://doi.org/10.1158/1055-9965.EPI-05-0368.

54. Gaikwad NW, Yang L, Weisenburger DD, Vose J, Beseler C, Rogan EG, et al. Urinary biomarkers suggest that estrogen-DNA adducts may play a role in the aetiology of non-Hodgkin lymphoma. Biomarkers. 2009;14:502-12, https://doi.org/10.3109/13547500903121715.

55. Zhang Y, Yue L, Nie Z, Chen J, Guo L, Wu B, et al. Simultaneous determination of four sulfur mustard-DNA adducts in rabbit urine after dermal exposure by isotope-dilution liquid chromatography-tandem mass spectrometry. J Chromatogr B Analyt Technol Biomed Life Sci. 2014;961:29-35, https://doi.org/10.1016/j.jchromb.2014.04.050.

56. Roser M, Beal D, Eldin C, Gudimard L, Caffin F, Gros-Desormeaux F, et al. Glutathione conjugates of the mercapturic acid pathway and guanine adduct as biomarkers of exposure to CEES, a sulfur mustard analog. Anal Bional Chem. 2021;413:1337–51, https://doi.org/10.1007/s00216-020-03096-4.

57. Henriksen T, Weimann A, Larsen EL, Poulsen HE. Quantification of 8-oxo-7,8-dihydro-2 '-deoxyguanosine and 8-oxo-7,8-di-hydro-guanosine concentrations in urine and plasma for estimating 24-h urinary output. Free Radic Biol Med. 2021;172:350-7, https://doi.org/10.1016/j.freeradbiomed.2021.06.014.

58. Gan W, Liu X-L, Yu T, Zou Y-G, Li T-T, Wang S, et al. Urinary 8-oxo-7,8-dihydroguanosine as a potential biomarker of aging. Front Aging Neurosci. 2018;10, https://doi.org/10.3389/fnagi.2018.00034.

59. Zanolin ME, Girardi P, Degan P, Rava M, Olivieri M, Di Gennaro G, et al. Measurement of a urinary marker (8-hydroxydeoxy-guanosine, 8-OHdG) of DNA oxidative stress in

epidemiological surveys: a pilot study. Int J Biol Markers. 2015;30:E341-E5, https://doi.org/10.5301/jbm.5000129.

60. Douki T, Sage E. Dewar valence isomers, the third type of environmentally relevant DNA photoproducts induced by solar radiation. Photochem Photobiol Sci. 2015;15:24-30, https://doi.org/10.1039/c5pp00382b.

61. Douki T. Low ionic strength reduces cytosine photoreactivity in UVC-irradiated isolated DNA. Photochem Photobiol Sci. 2006;5:1045-51, https://doi.org/http://dx.doi.org/10.1039/b604517k.

62. Hosszu JL, Rahn RO. Thymine dimer formation in DNA between 25°C and 100°C. Biochem Biophys Res Com. 1967;29:327-30, https://doi.org/10.1016/0006-291X(67)90457-3.

63. Douki T. Effect of denaturation on the photochemistry of pyrimidine bases in isolated DNA. J Photochem Photobiol B: Biol. 2006;82:45-52, https://doi.org/http://dx.doi.org/10.1016/j.photobiol.2005.08.009.